

# Supporting Information: Defect Tolerance in Monolayer Transition Metal Dichalcogenides

Mohnish Pandey,<sup>†</sup> Filip A. Rasmussen,<sup>†</sup> Korina Kuhar,<sup>†</sup> Thomas Olsen,<sup>†</sup> Karsten  
W. Jacobsen,<sup>†</sup> and Kristian S. Thygesen<sup>\*,†,‡</sup>

*Center for Atomic-scale Materials Design, Department of Physics, Technical University of  
Denmark, DK - 2800 Kongens Lyngby, Denmark, and Center for Nanostructured Graphene  
(CNG), Department of Physics, Technical University of Denmark, DK - 2800 Kongens  
Lyngby, Denmark*

E-mail: thygesen@fysik.dtu.dk

---

\*To whom correspondence should be addressed

<sup>†</sup>Center for Atomic-scale Materials Design, Department of Physics, Technical University of Denmark, DK  
- 2800 Kongens Lyngby, Denmark

<sup>‡</sup>Center for Nanostructured Graphene (CNG), Department of Physics, Technical University of Denmark,  
DK - 2800 Kongens Lyngby, Denmark

# Calculations without relaxation of the vacancies:

In this section all the band structures correspond to the case of unrelaxed and neutral defects.

## Defect tolerant 1T monolayers:

The band structures plotted below correspond to the defect tolerant 1T structures. The left panel in all the plots corresponds to the pristine structure in a  $3 \times 3$  unit cell. The right panel corresponds to the defect structure in which one chalcogen atom is removed from a  $3 \times 3$  unit cell. The removal of the chalcogen atom introduces only shallow state(s) in the band gap. Density of states (DOS) is also shown in order to show the nature of the states present in the valence and conduction band.

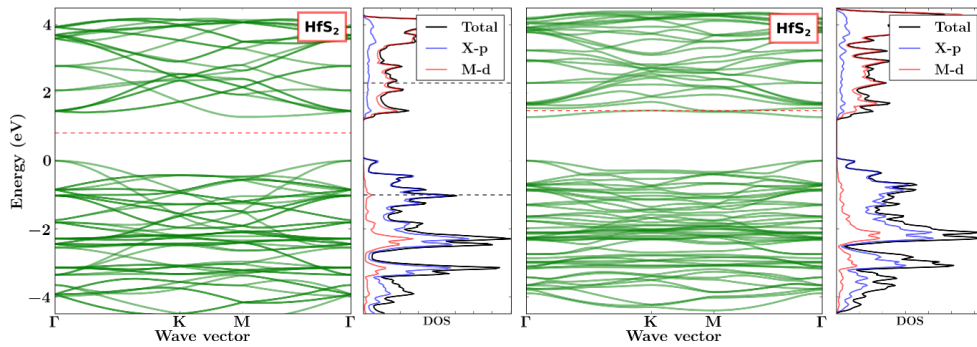


Figure S1

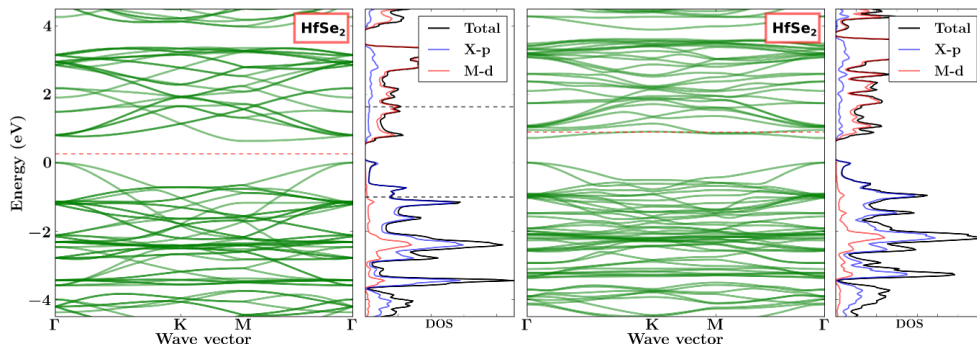


Figure S2

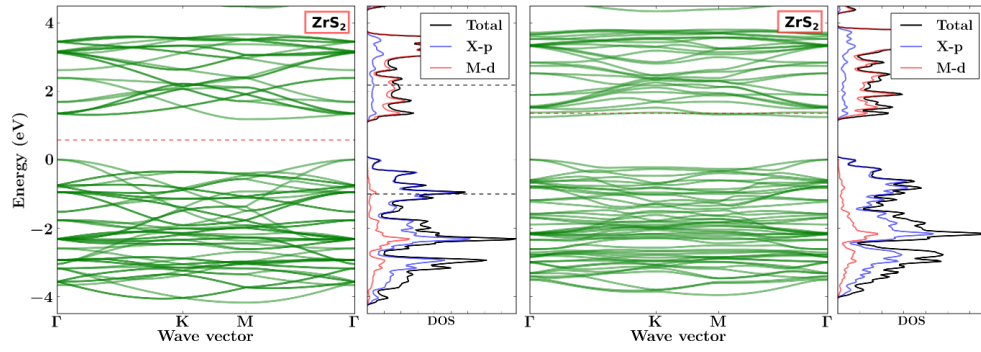


Figure S3

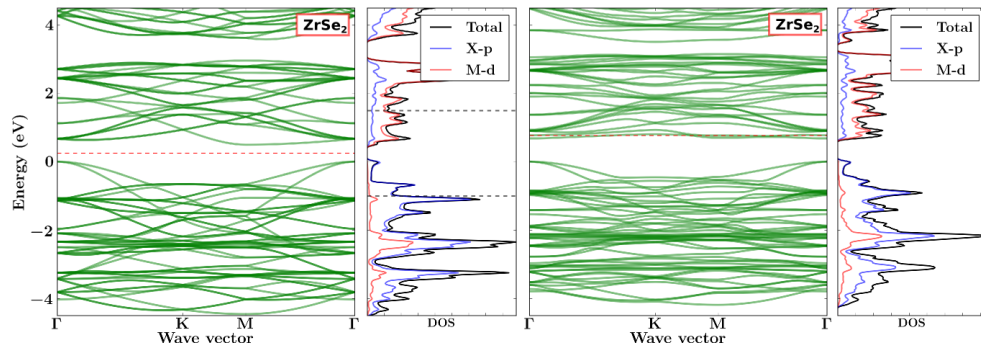


Figure S4

## Defect tolerant 2H monolayers:

The band structures plotted below correspond to the defect tolerant 2H structures. The left panel in all the plots corresponds to the pristine structure in a  $3\times 3$  unit cell. The right panel corresponds to the defect structure in which one chalcogen atom is removed from a  $3\times 3$  unit cell. The removal of the chalcogen atom introduces only shallow state(s) in the band gap. Density of states (DOS) is also shown in order to show the nature of the states present in the valence and conduction band.

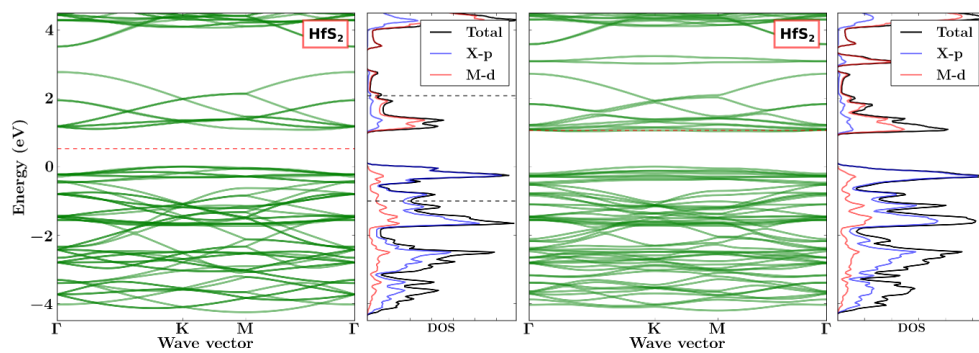


Figure S5

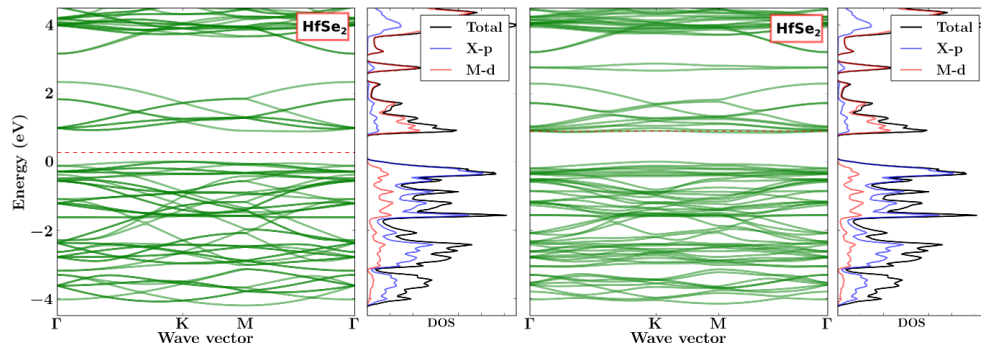


Figure S6

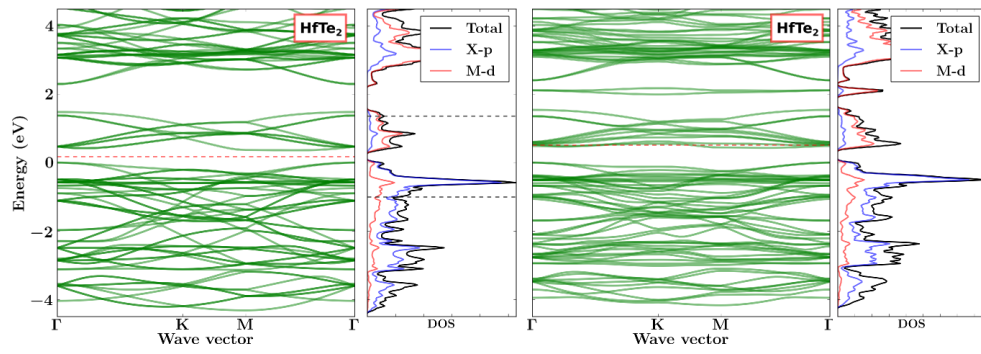


Figure S7

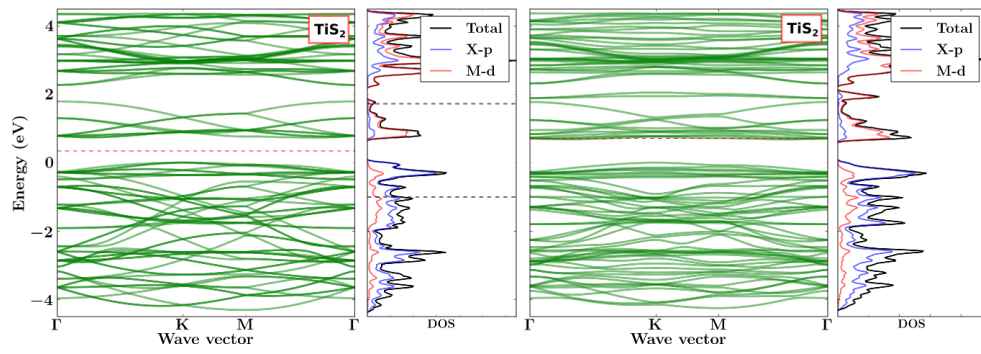


Figure S8

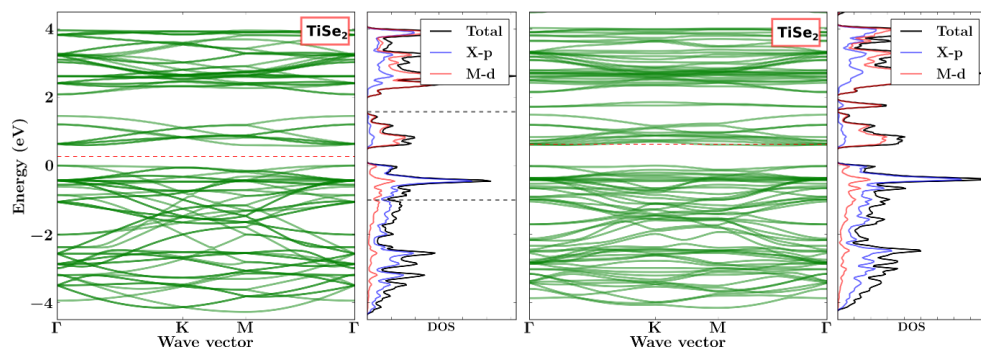


Figure S9

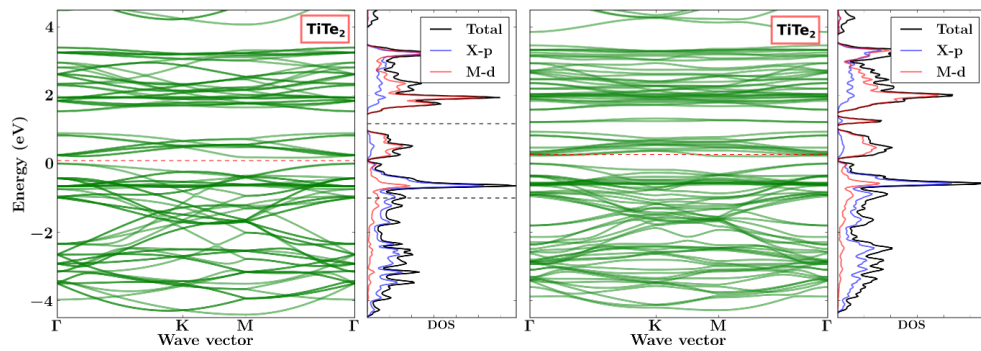


Figure S10

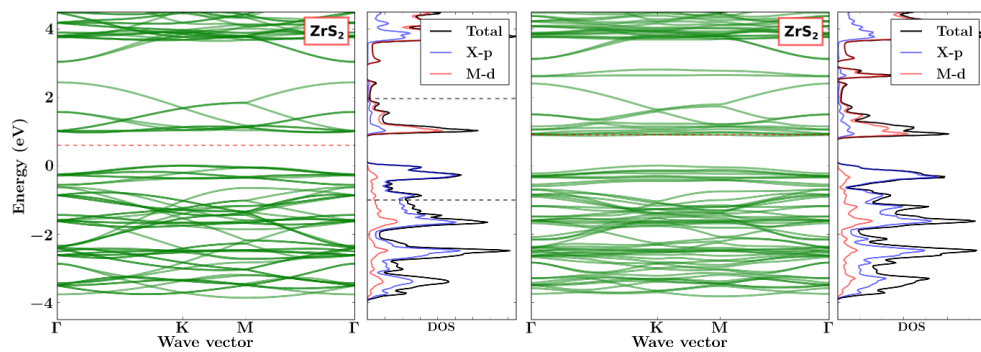


Figure S11

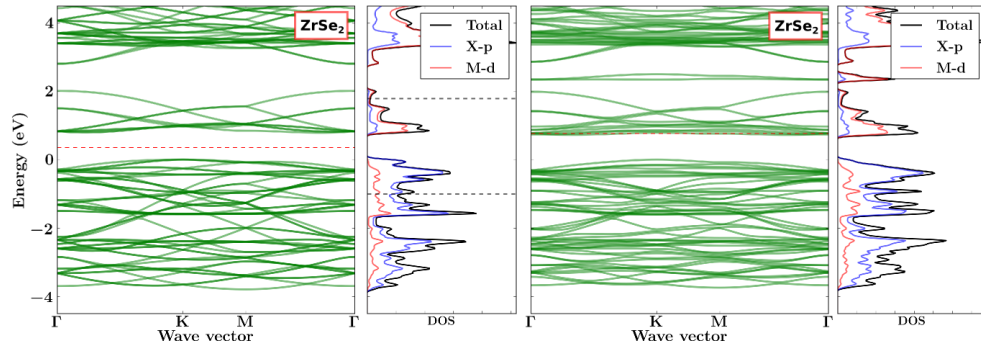


Figure S12

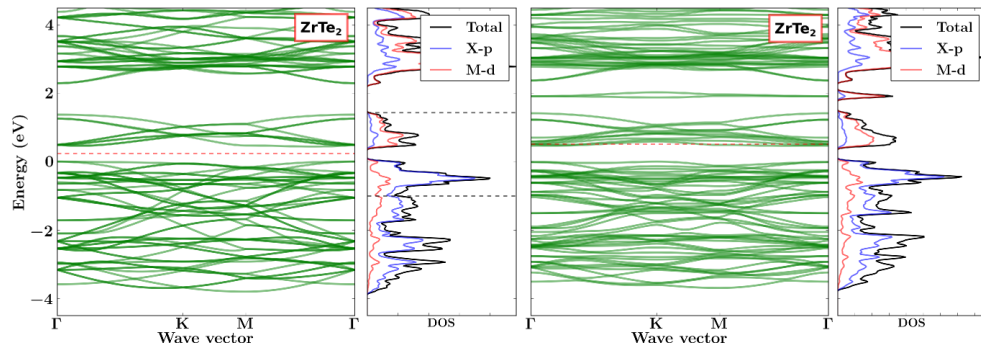


Figure S13

## Defect sensitive 1T monolayers:

The band structures plotted below correspond to the defect sensitive 1T structures. The left panel in all the plots corresponds to the pristine structure in a  $3\times 3$  unit cell. The right panel corresponds to the defect structure in which one chalcogen atom is removed from a  $3\times 3$  unit cell. The removal of the chalcogen atom introduces deep state(s) in the band gap. Density of states (DOS) is also shown in order to show the nature of the states present in the valence and conduction band.

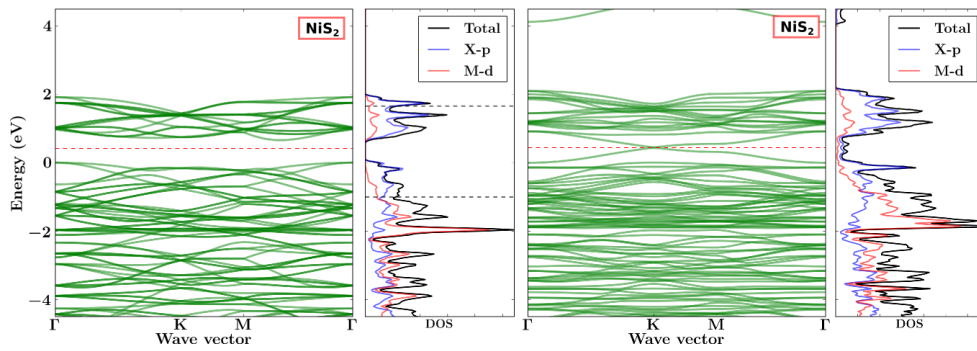


Figure S14

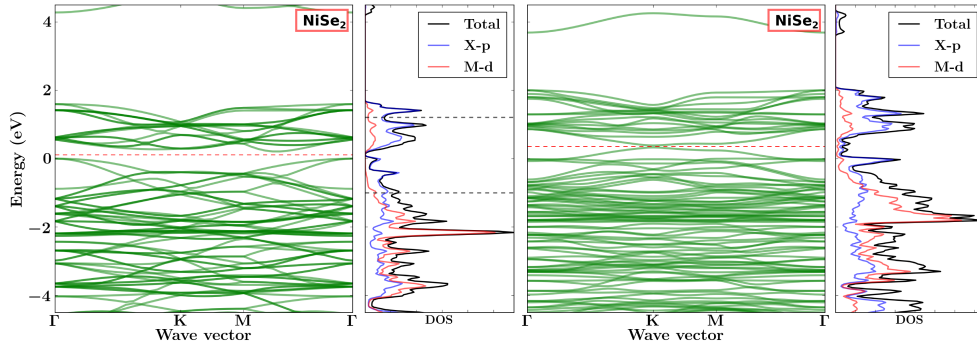


Figure S15

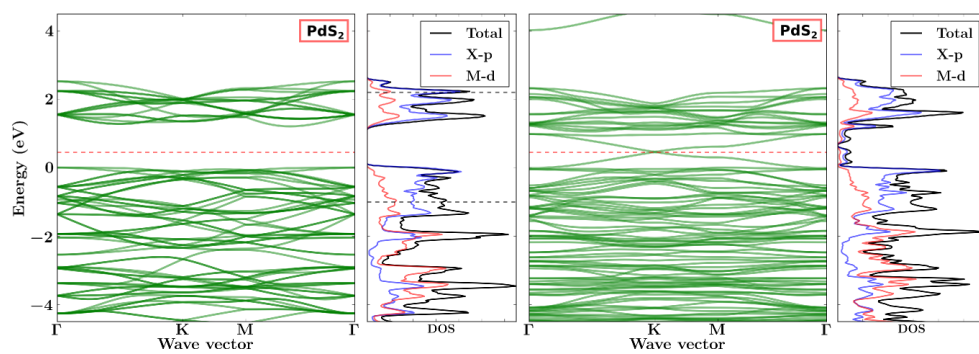


Figure S16

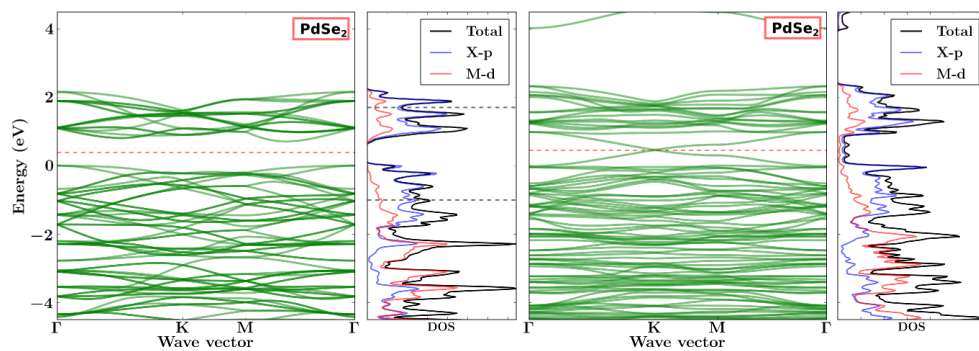


Figure S17

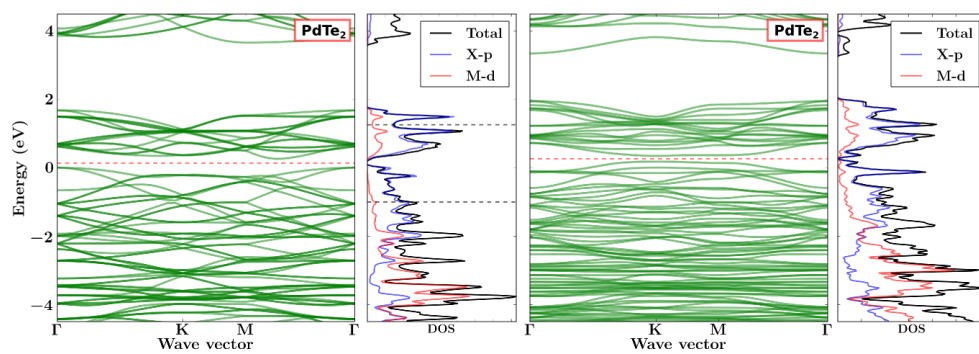


Figure S18

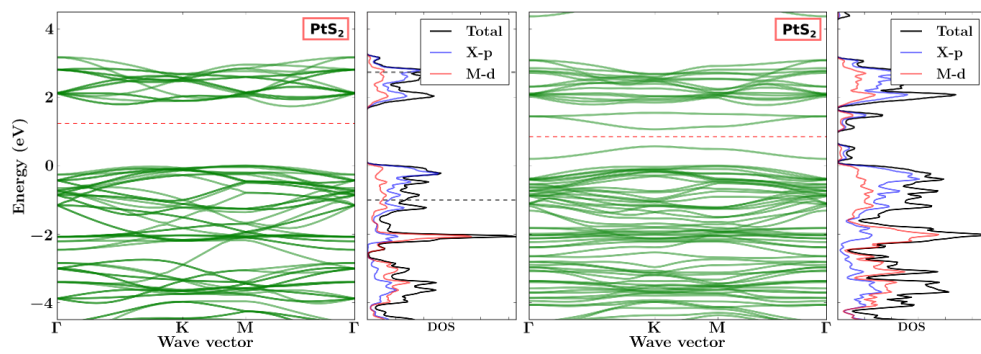


Figure S19

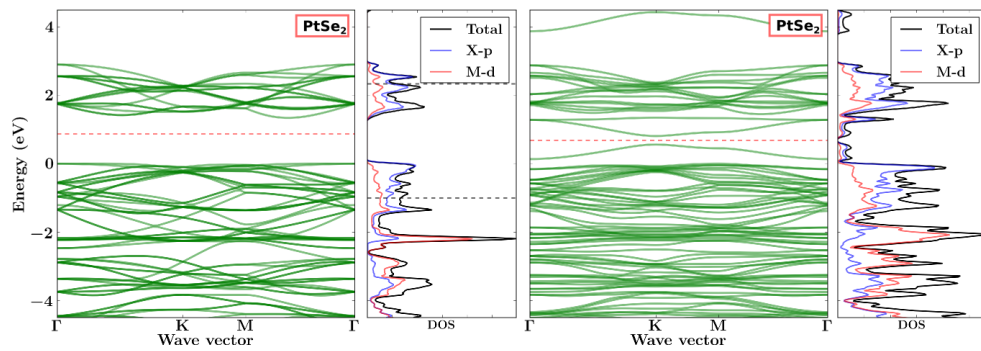


Figure S20

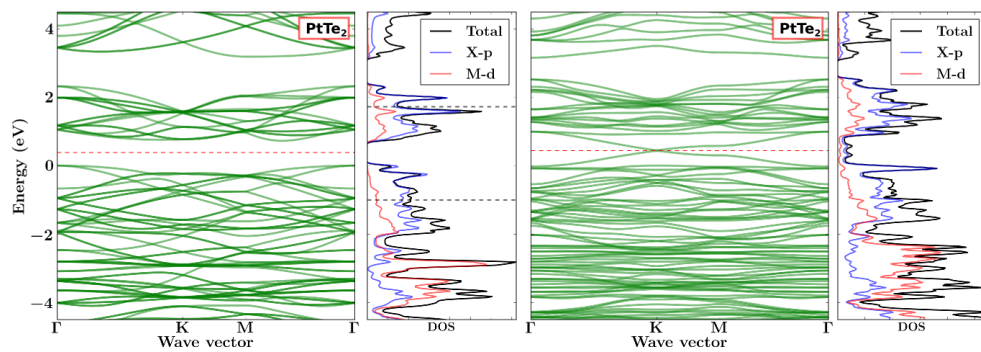


Figure S21

## Defect sensitive 2H monolayers:

The band structures plotted below correspond to the defect sensitive 2H structures. The left panel in all the plots corresponds to the pristine structure in a  $3\times 3$  unit cell. The right panel corresponds to the defect structure in which one chalcogen atom is removed from a  $3\times 3$  unit cell. The removal of the chalcogen atom introduces deep state(s) in the band gap. Density of states (DOS) is also shown in order to show the nature of the states present in the valence and conduction band.

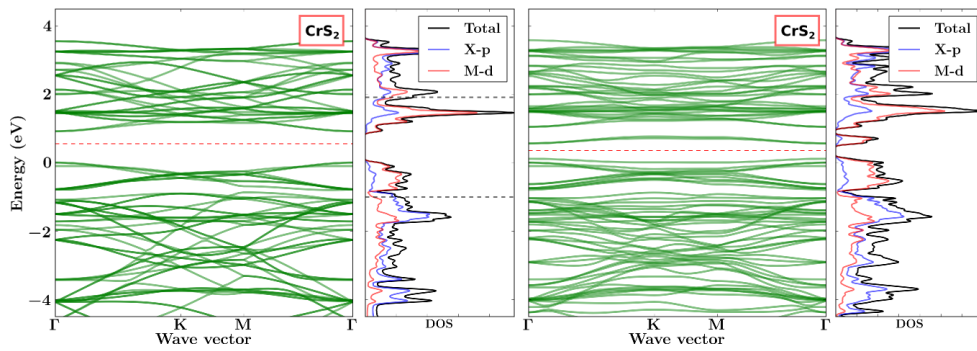


Figure S22

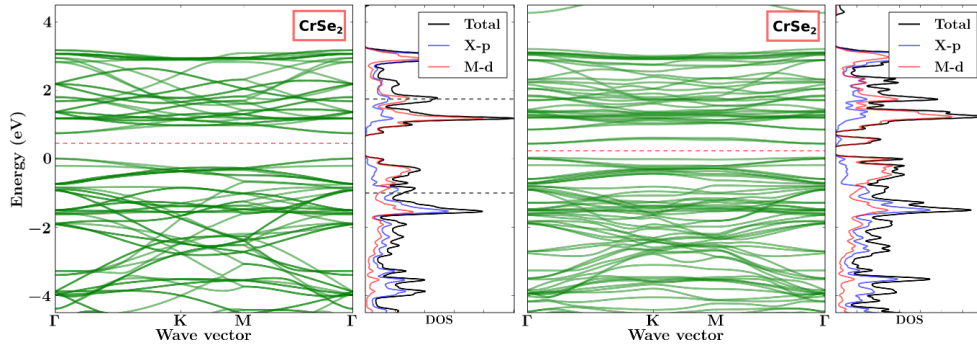


Figure S23

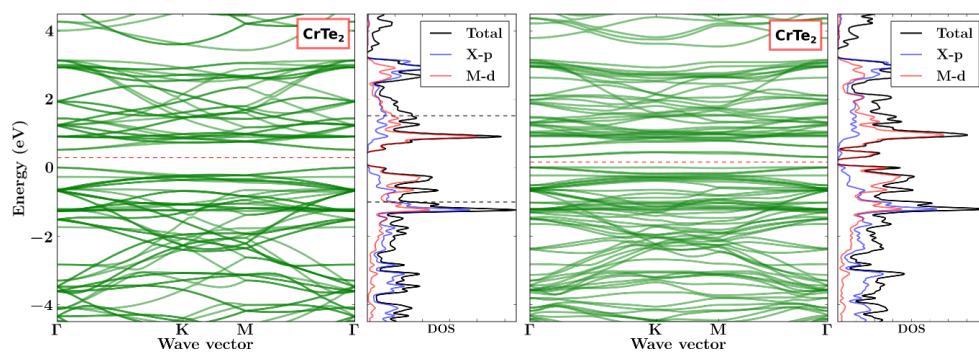


Figure S24

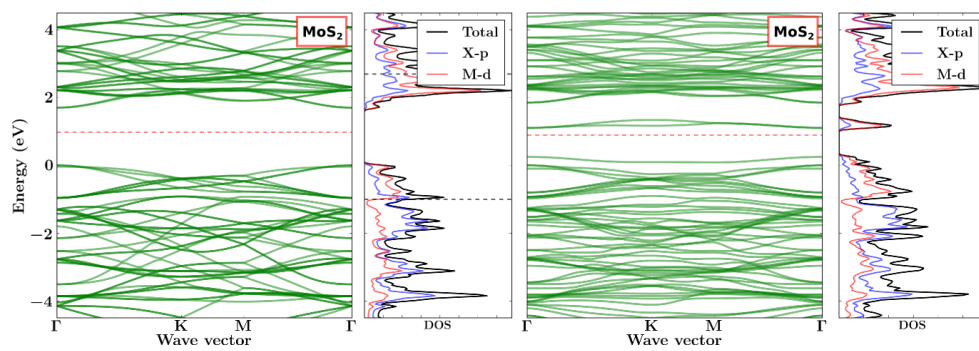


Figure S25

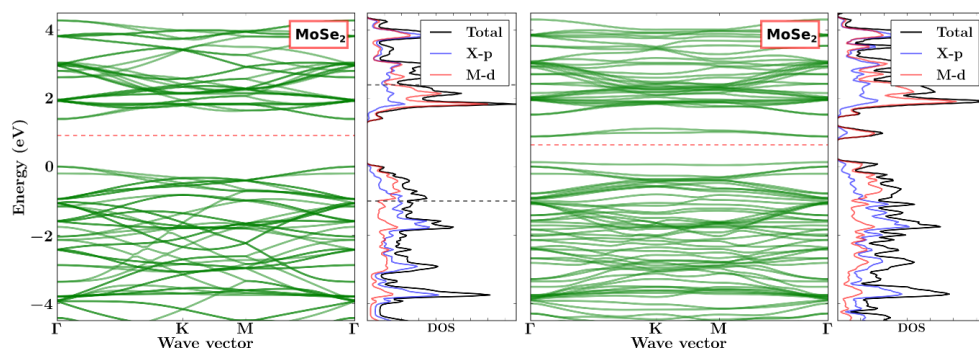


Figure S26

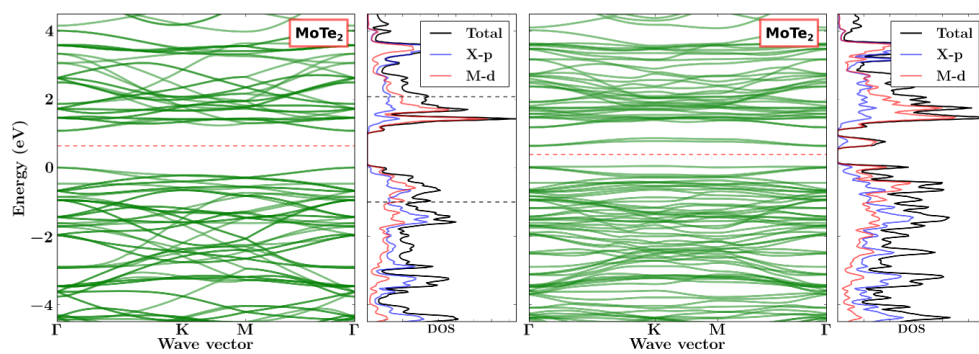


Figure S27

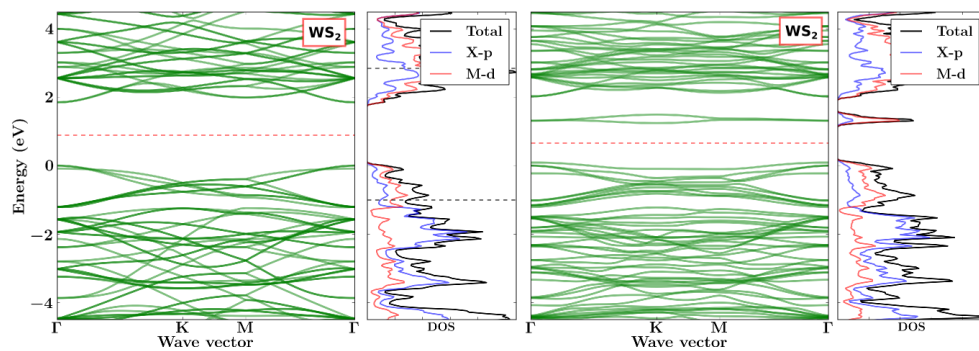


Figure S28

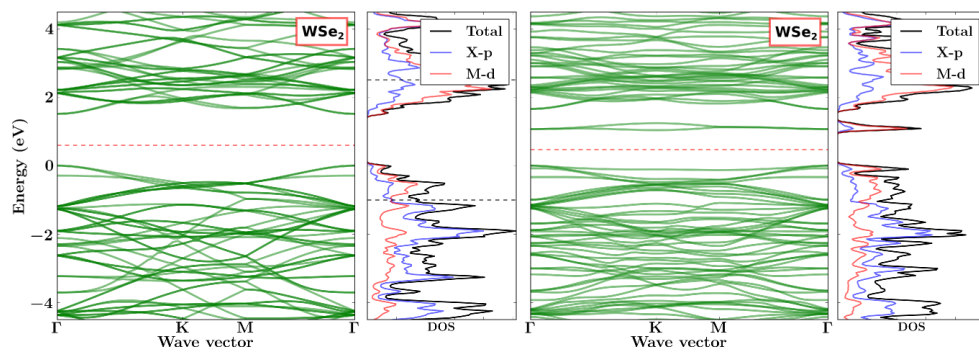


Figure S29

# Calculation of edge state in non-polar nanoribbons:

## 1T shallow edge states:

The plots on the left panel correspond to the pristine monolayer metal dichalcogenides. The right panel show the band structure of the nanoribbons cleaved from the monolayer along the non-polar direction. In the defect tolerant 1T monolayers, only shallow edge states are introduced when the monolayer is cleaved along the non-polar direction.

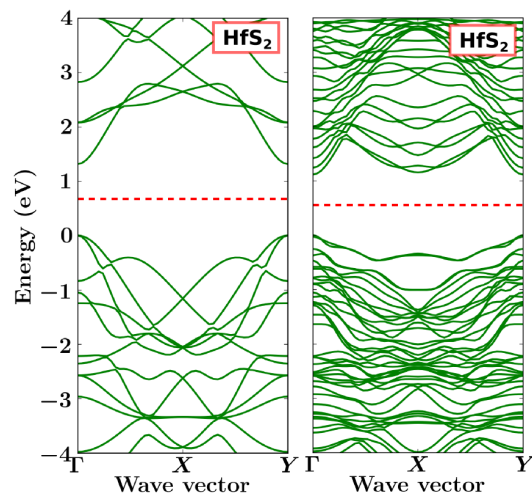


Figure S30

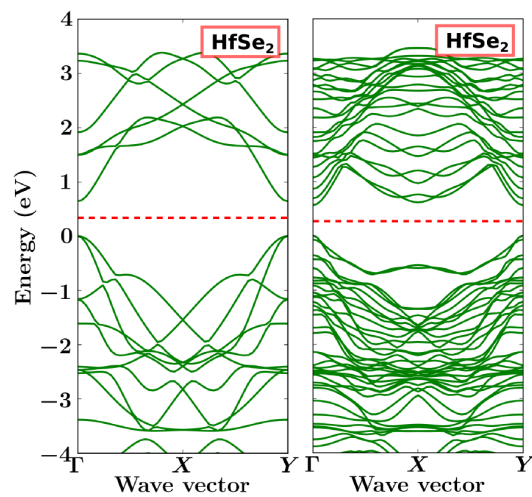


Figure S31

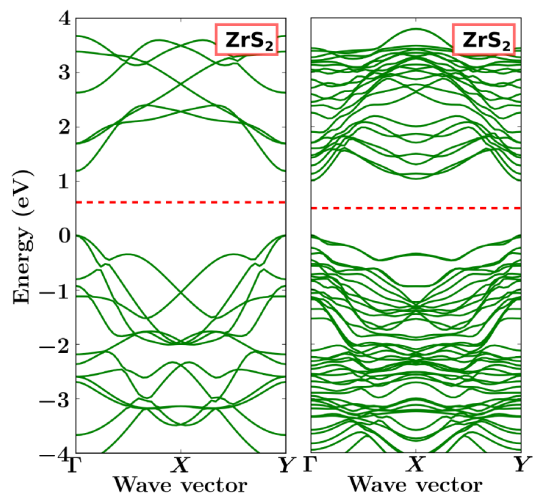


Figure S32

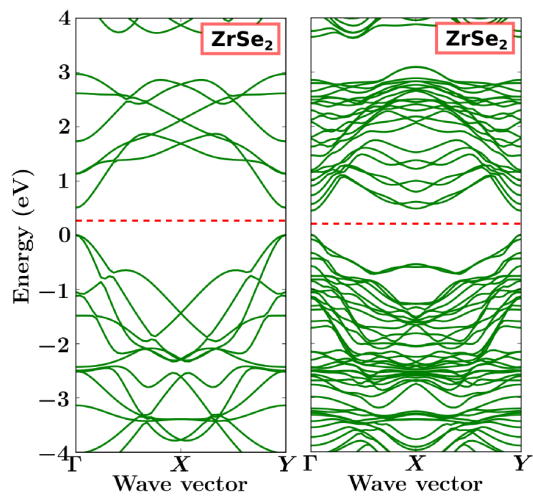


Figure S33

## 2H shallow edge states:

The plots on the left panel correspond to the pristine monolayer metal dichalcogenides. The right panel show the band structure of the nanoribbons cleaved from the monolayer along the non-polar direction. In the defect tolerant 2H monolayers, only shallow edge states are introduced when the monolayer is cleaved along the non-polar direction.

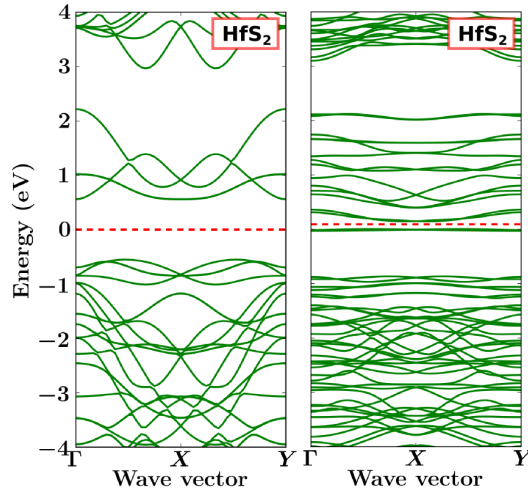


Figure S34

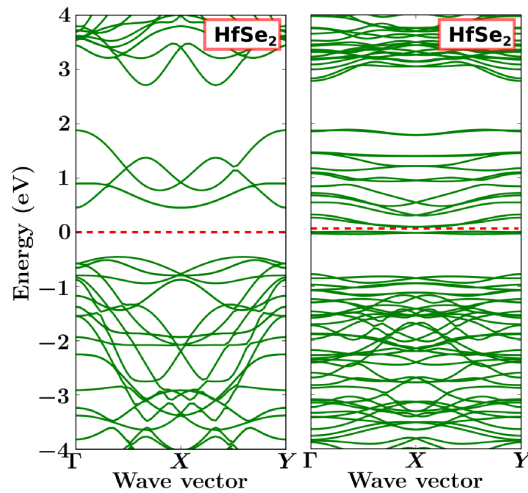


Figure S35

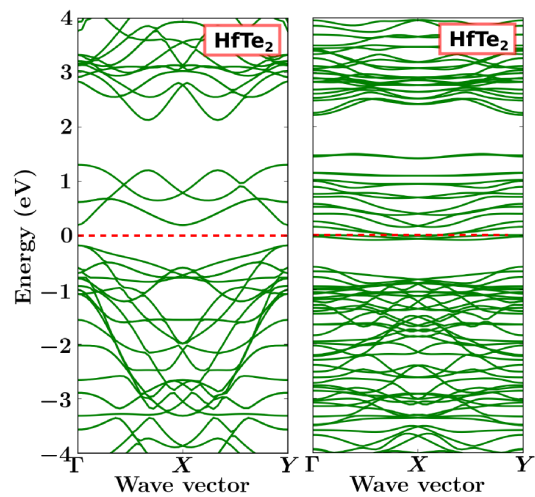


Figure S36

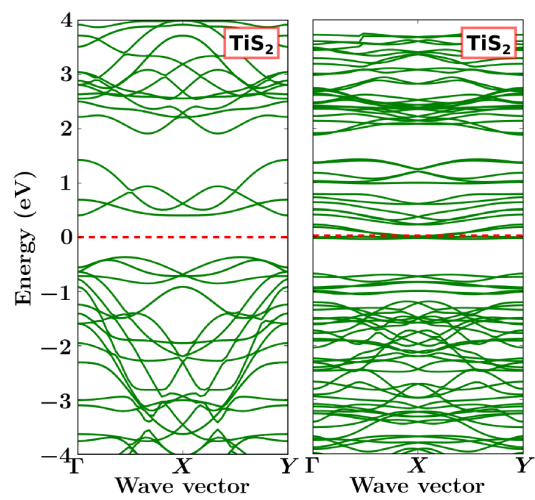


Figure S37

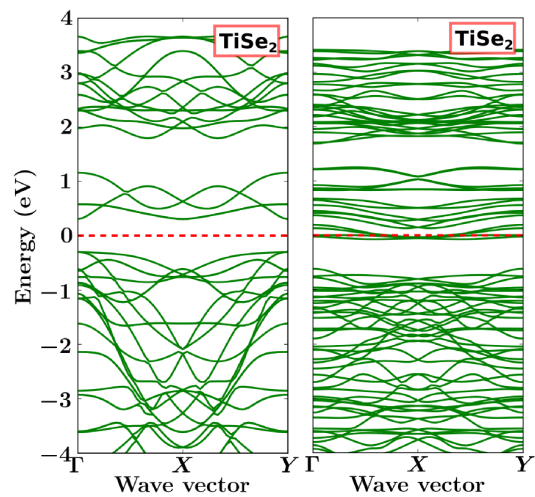


Figure S38

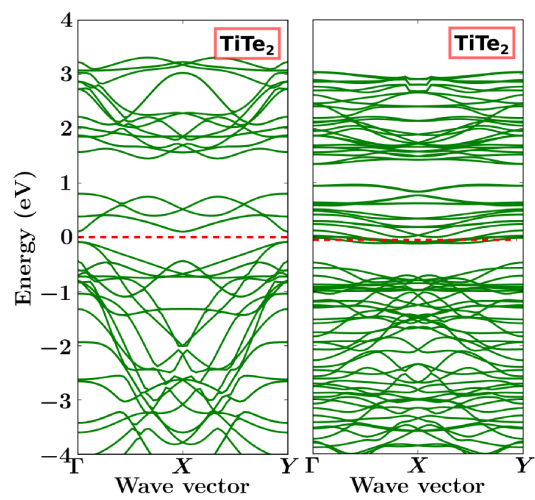


Figure S39

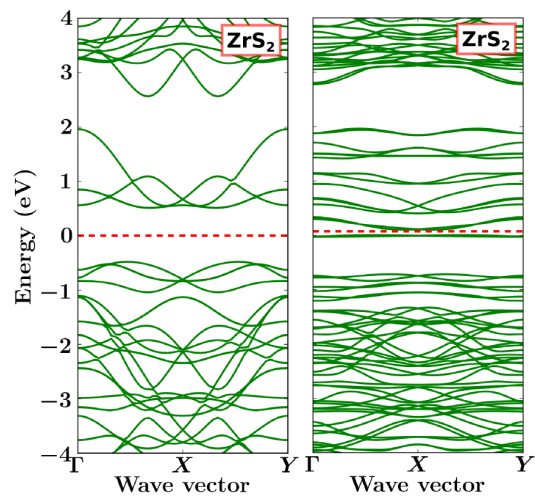


Figure S40

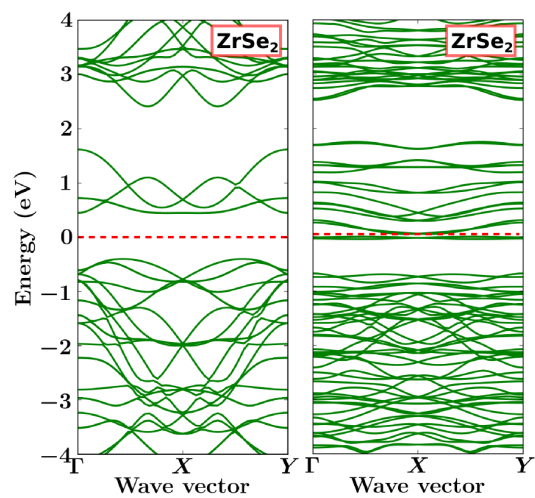


Figure S41

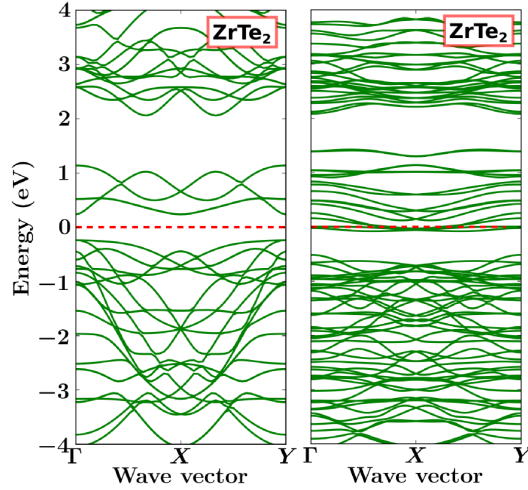


Figure S42

### 1T mid-gap edge states:

The plots on the left panel correspond to the pristine monolayer metal dichalcogenides. The right panel show the band structure of the nanoribbons cleaved from the monolayer along the non-polar direction. In the defect sensitive 1T monolayers, deep gap states are introduced when the monolayer is cleaved along the non-polar direction.

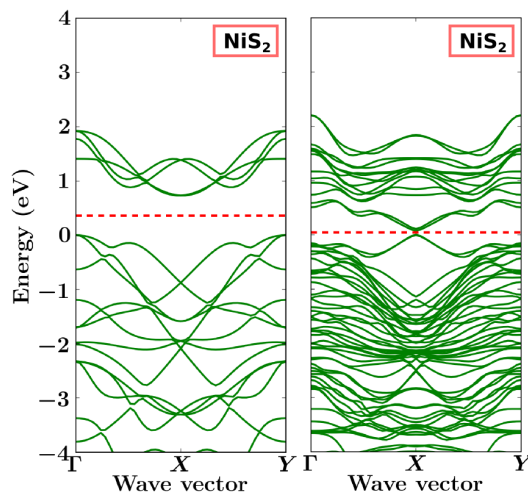


Figure S43

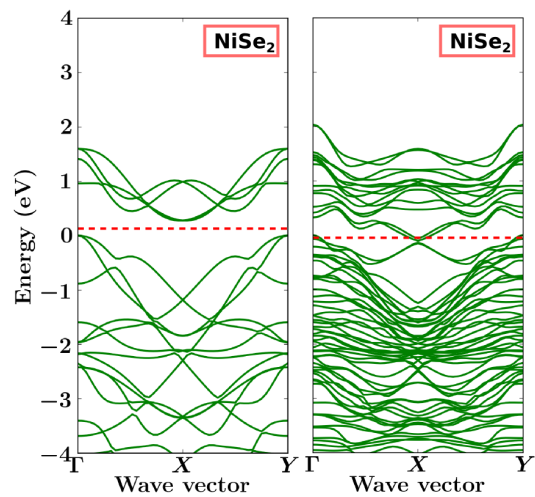


Figure S44

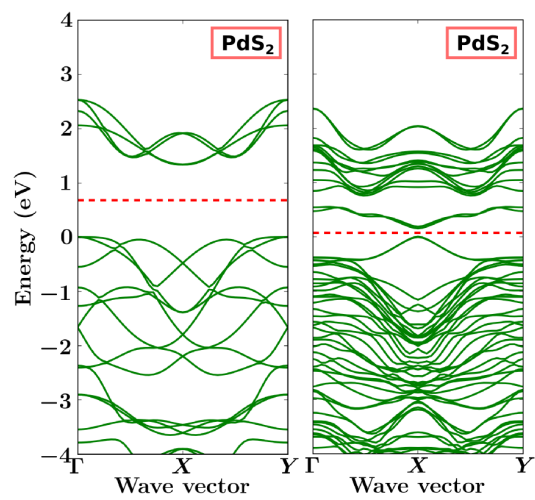


Figure S45

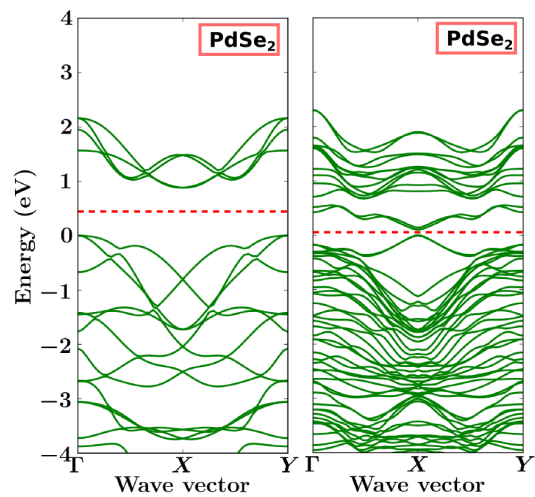


Figure S46

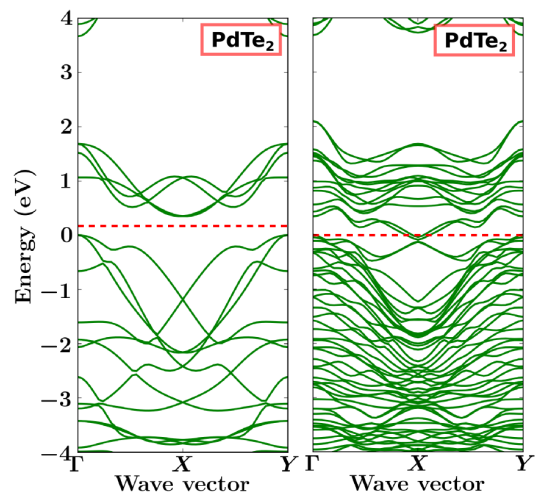


Figure S47

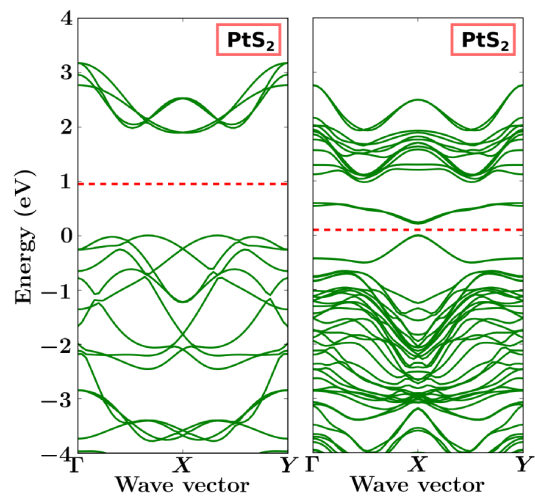


Figure S48

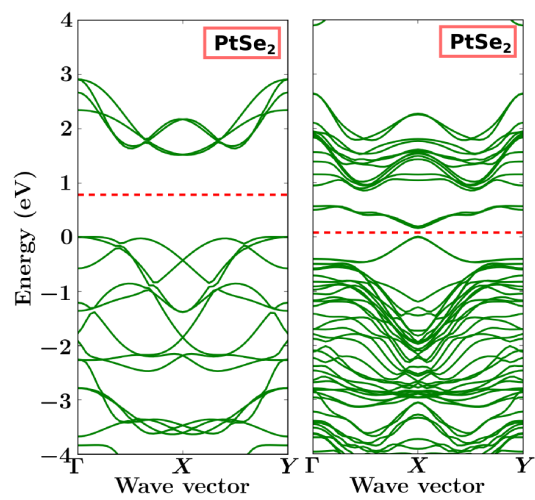


Figure S49

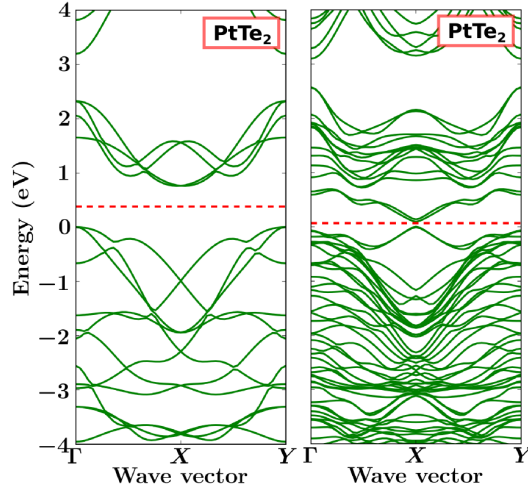


Figure S50

## 2H mid-gap edge states:

The plots on the left panel correspond to the pristine monolayer metal dichalcogenides. The right panel show the band structure of the nanoribbons cleaved from the monolayer along the non-polar direction. In the defect sensitive 2H monolayers, deep gap states are introduced when the monolayer is cleaved along the non-polar direction.

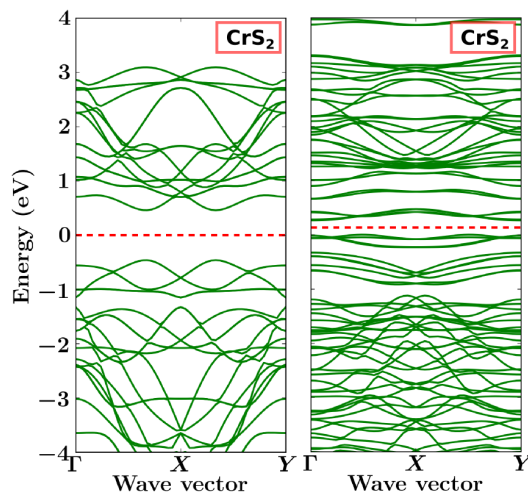


Figure S51

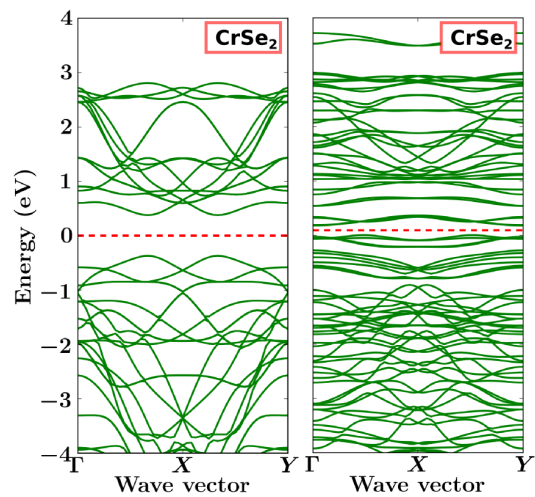


Figure S52

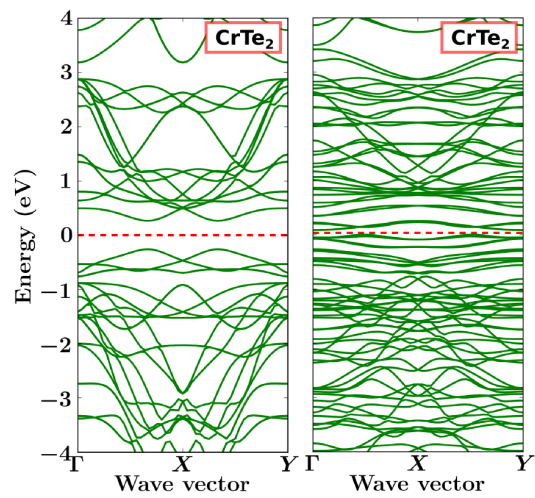


Figure S53

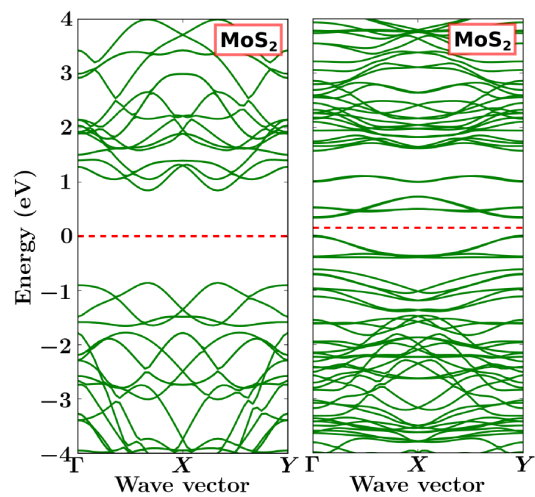


Figure S54

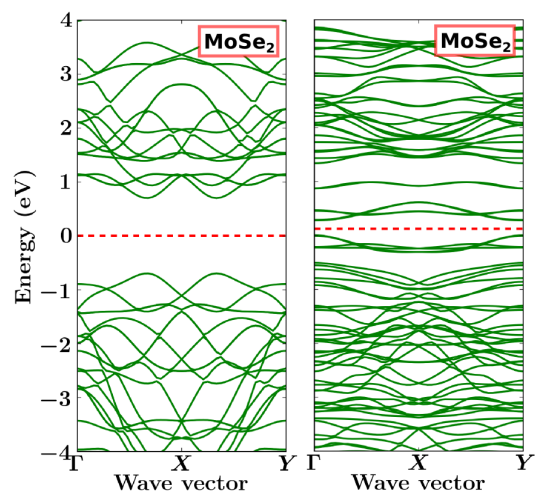


Figure S55

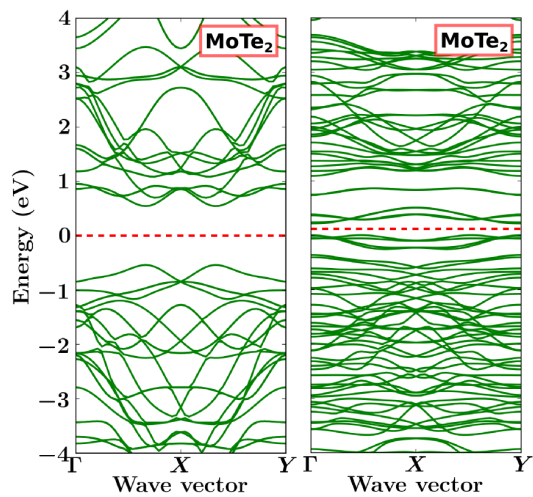


Figure S56

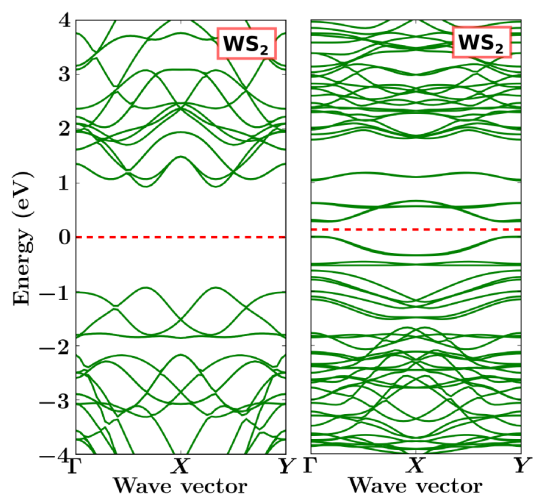


Figure S57

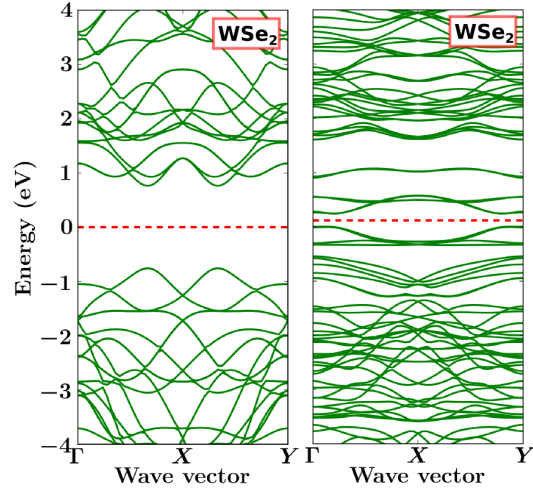


Figure S58

Dependence of the descriptor on the energy window:

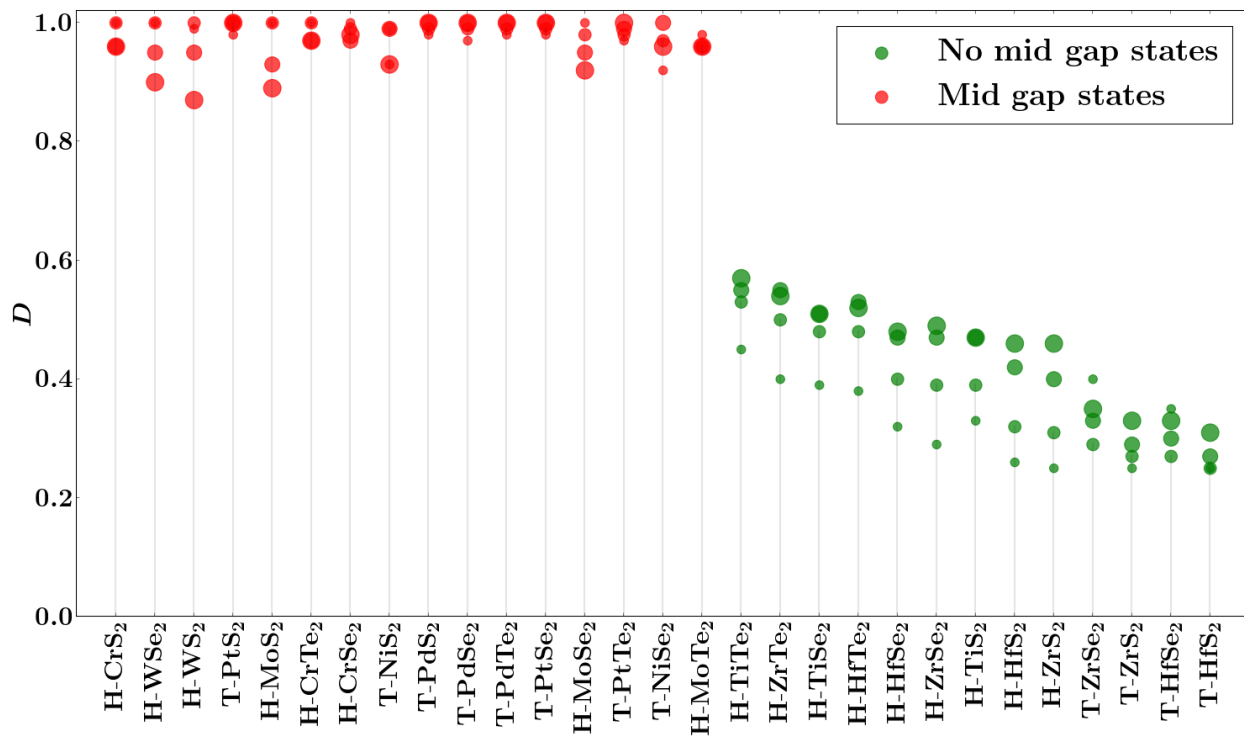


Figure S59: Descriptor for different energy window used for integration. Compounds have been sorted based on the value of descriptor obtained using an energy window of 1 eV. The increasing size of the circle represent the energy window of 0.5, 1.0, 1.5 and 2.0 eV respectively. In some cases the ordering of the compounds is different from the main text because the compounds have the same value of the descriptor thus making the sorting a bit arbitrary.

## **Effect of structural relaxation and charging of the supercell:**

In this section we show how structural relaxation and changing the charge state of the defects influence the band structure and projected density of states for a representative set of TMDs comprised by two materials from each of the three classes shown in the abstract graphics.

### **Defect levels with of the neutral systems and the systems with added fractional charge:**

All the plots in the left panel show the band structure of the pristine systems with  $3 \times 3$  unit cell. The plots in the right panel corresponding to (a) represent systems with neutral vacancy without relaxation, (b) represent systems with neutral vacancy with relaxation, (c) represent systems with vacancy with  $0.5 e^-$  added to the system and relaxed afterwards and (d) represent systems with vacancy with  $1 e^-$  added to the system and relaxed afterwards.

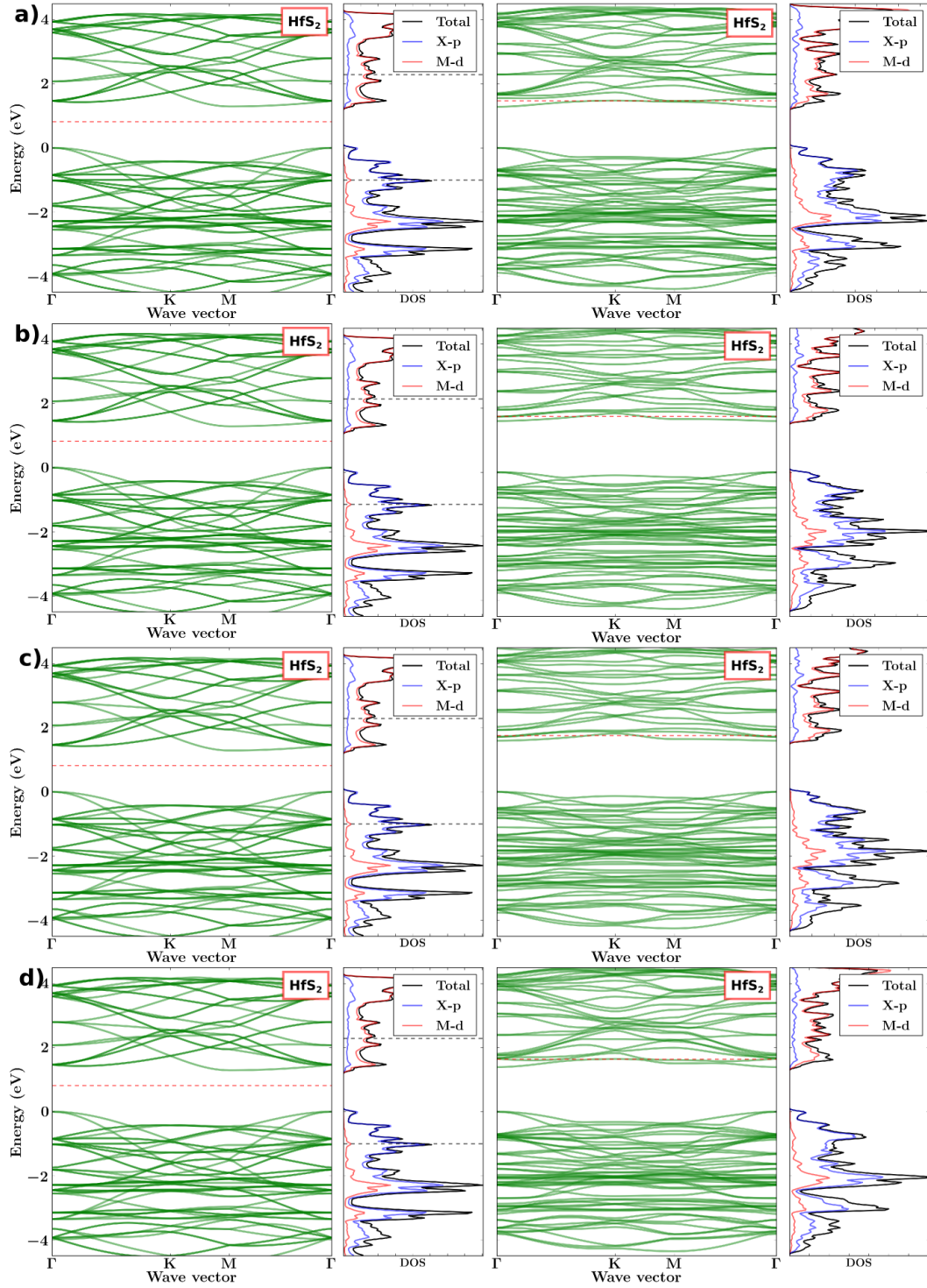


Figure S60: Effect of relaxation on the band structure of  $\text{HfS}_2$ . Left panel in all the subplots corresponds to the pristine structure. (a) No relaxation. (b) Relaxation of the of the neutral vacancy (c) Relaxation with  $0.5 e^-$  added to the system. (d) Relaxation with  $1 e^-$  added to the system.

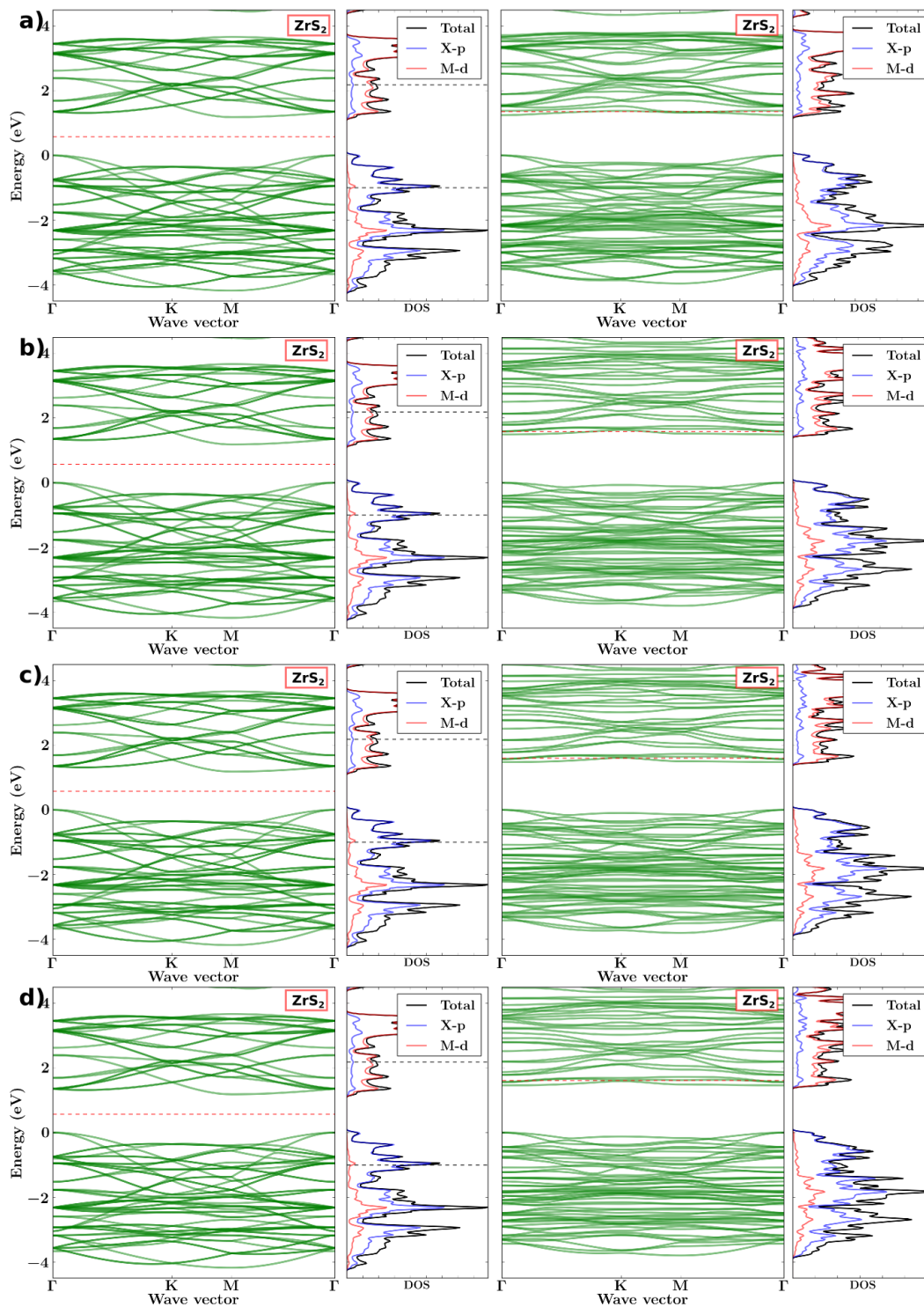


Figure S61: Effect of relaxation on the band structure of  $\text{ZrS}_2$ . Left panel in all the subplots corresponds to the pristine structure. (a) No relaxation. (b) Relaxation of the of the neutral vacancy (c) Relaxation with  $0.5 e^-$  added to the system. (d) Relaxation with  $1 e^-$  added to the system.

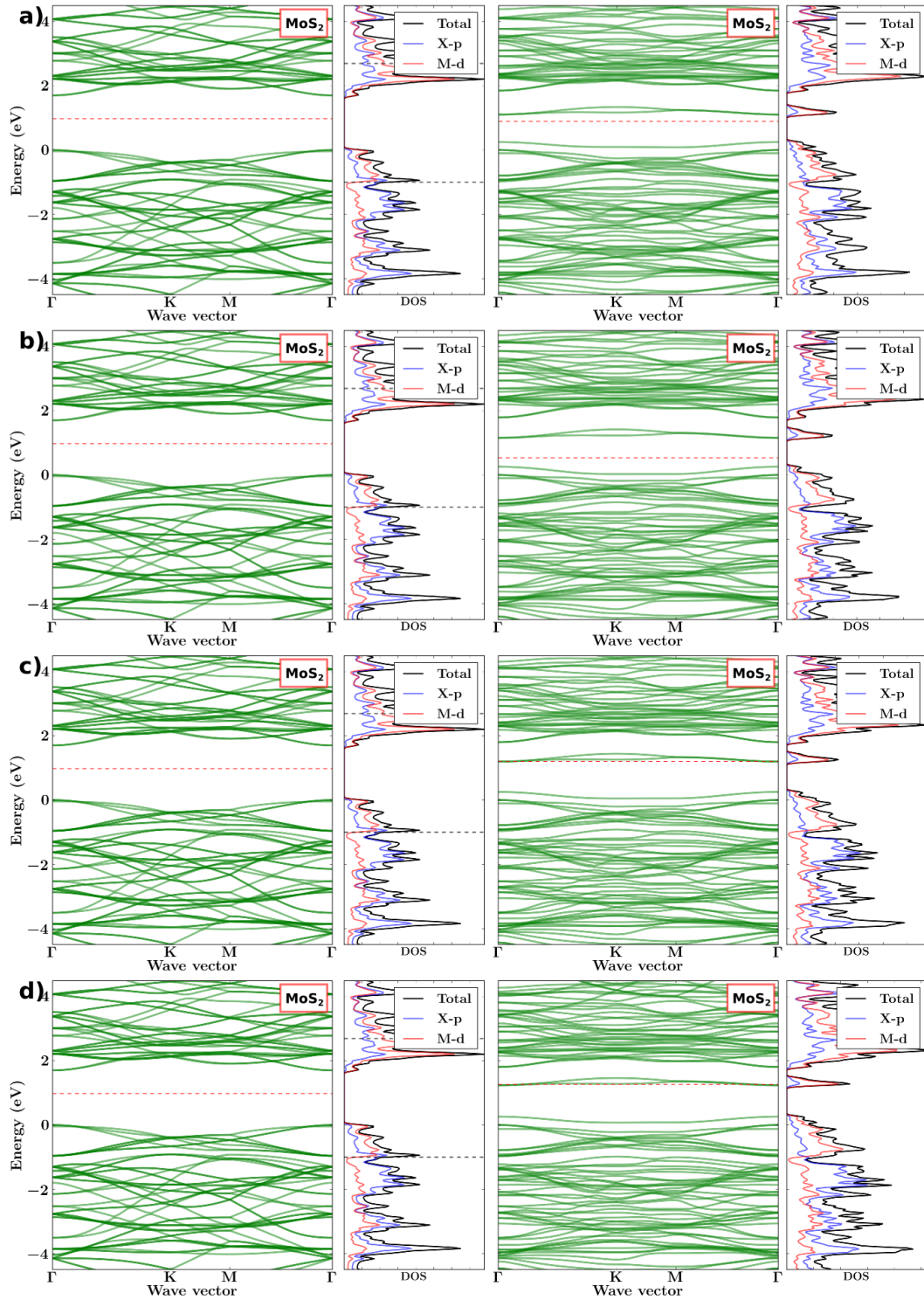


Figure S62: Effect of relaxation on the band structure of MoS<sub>2</sub>. Left panel in all the subplots corresponds to the pristine structure. (a) No relaxation. (b) Relaxation of the of the neutral vacancy (c) Relaxation with 0.5 e<sup>-</sup> added to the system. (d) Relaxation with 1 e<sup>-</sup> added to the system.

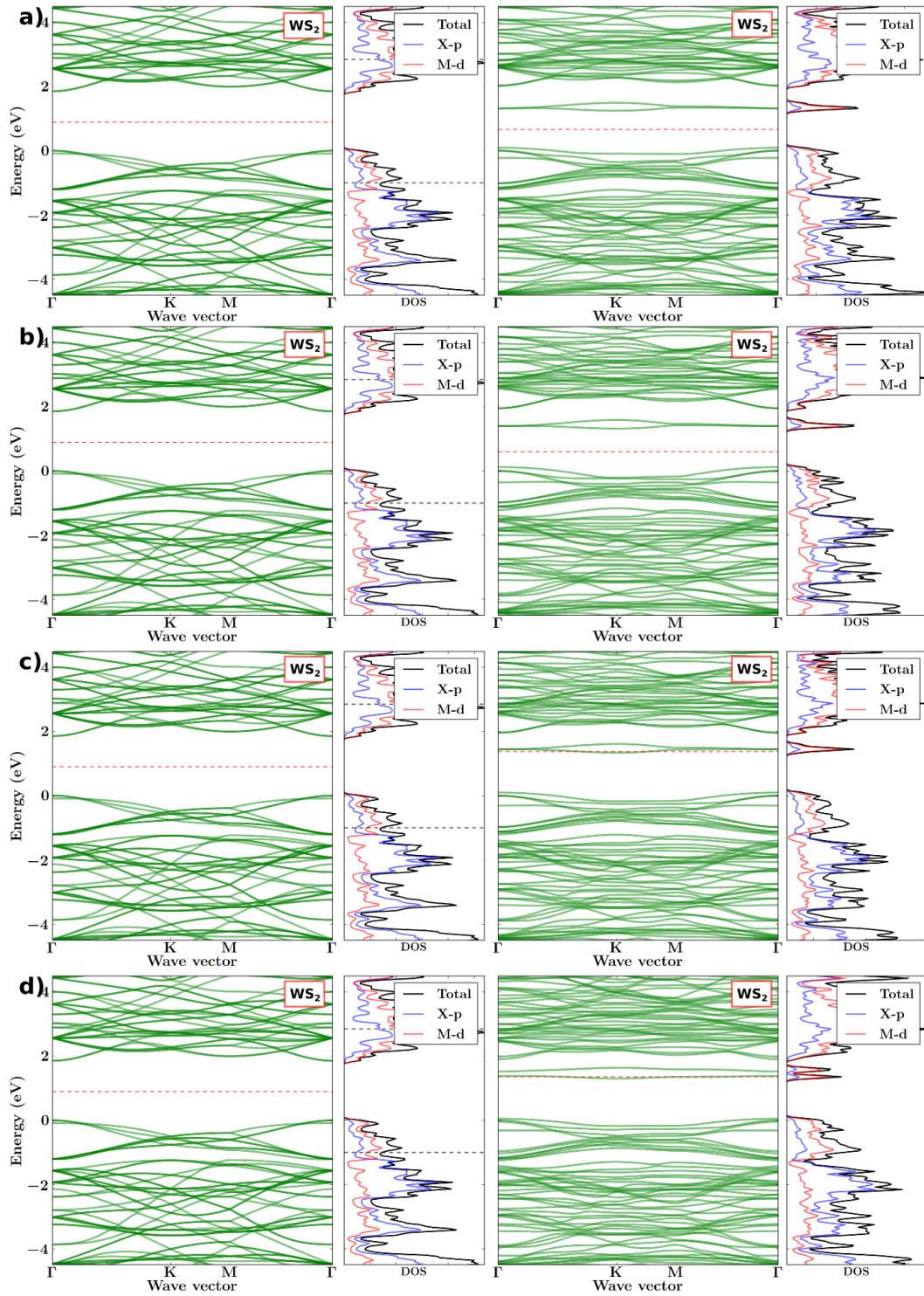


Figure S63: Effect of relaxation on the band structure of  $\text{WS}_2$ . Left panel in all the subplots corresponds to the pristine structure. (a) No relaxation. (b) Relaxation of the of the neutral vacancy (c) Relaxation with  $0.5 e^-$  added to the system. (d) Relaxation with  $1 e^-$  added to the system.

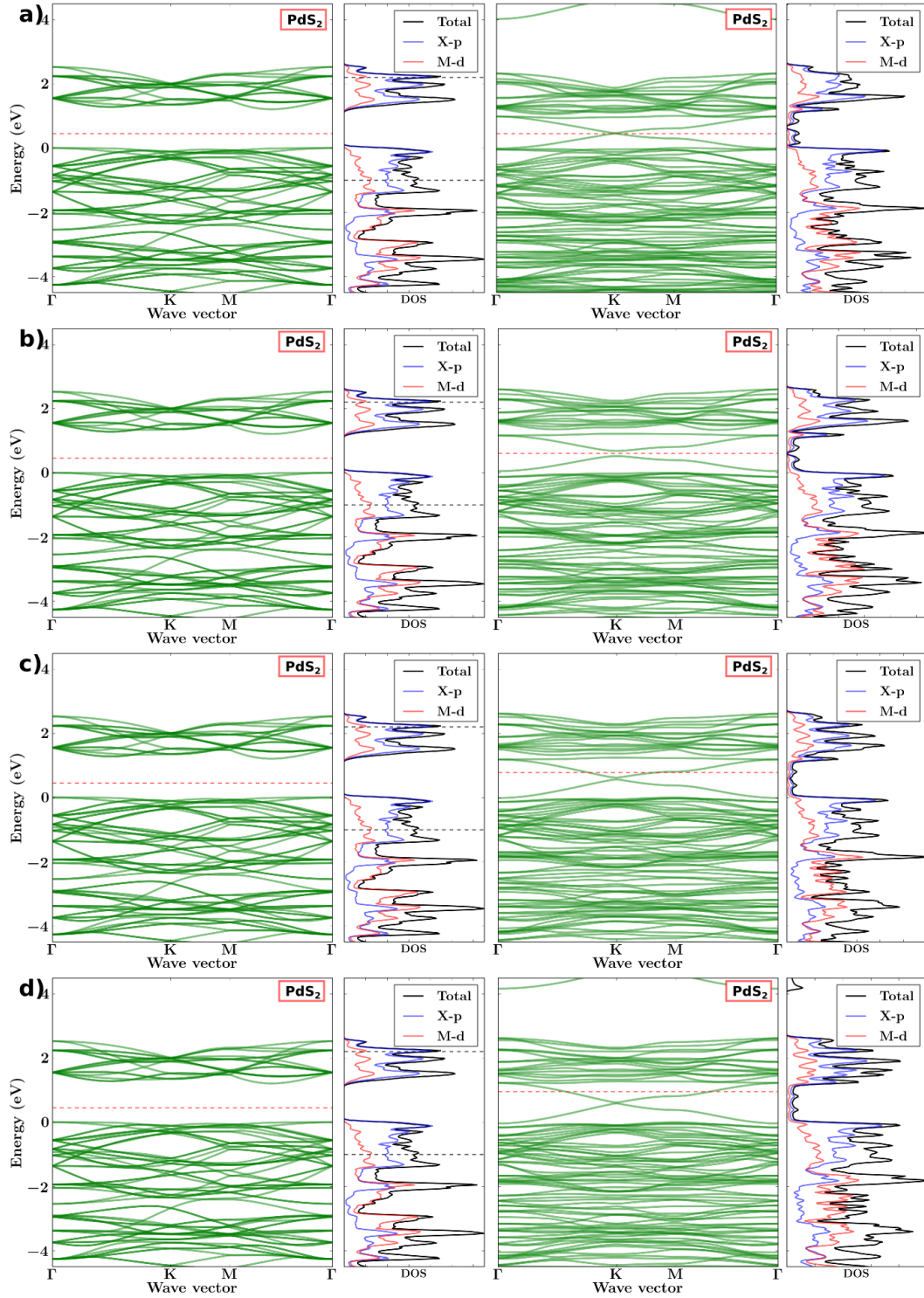


Figure S64: Effect of relaxation on the band structure of PdS<sub>2</sub>. Left panel in all the subplots corresponds to the pristine structure. (a) No relaxation. (b) Relaxation of the of the neutral vacancy (c) Relaxation with 0.5 e<sup>-</sup> added to the system. (d) Relaxation with 1 e<sup>-</sup> added to the system.

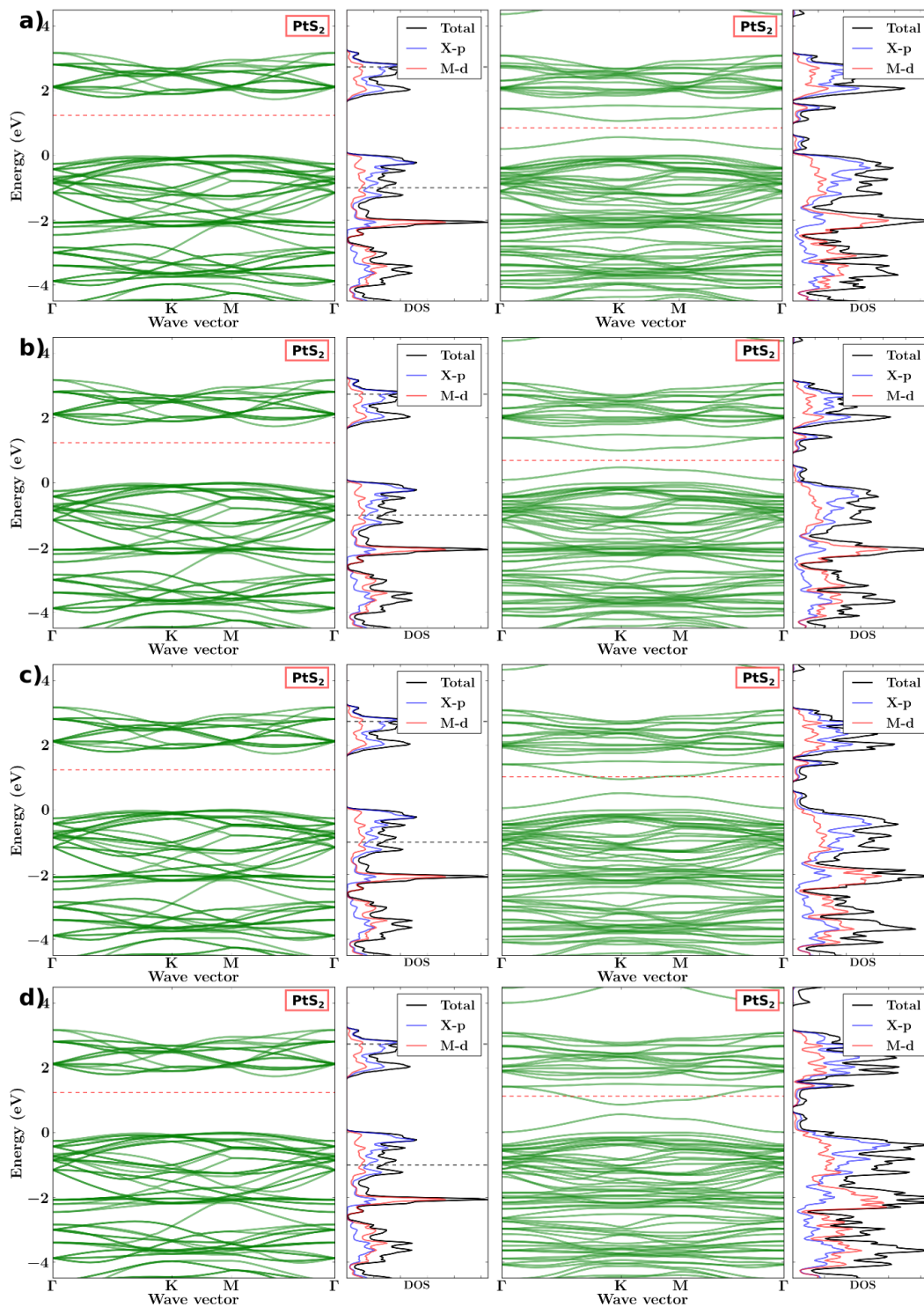


Figure S65: Effect of relaxation on the band structure of PtS<sub>2</sub>. Left panel in all the subplots corresponds to the pristine structure. (a) No relaxation. (b) Relaxation of the of the neutral vacancy (c) Relaxation with 0.5 e<sup>-</sup> added to the system. (d) Relaxation with 1 e<sup>-</sup> added to the system.

## Defect levels with removal of fractional charge:

The plots below show the comparison of the density of states of the representative systems with chalcogen vacancy in neutral supercell and with  $0.5 e^-$  removed and relaxed afterwards.

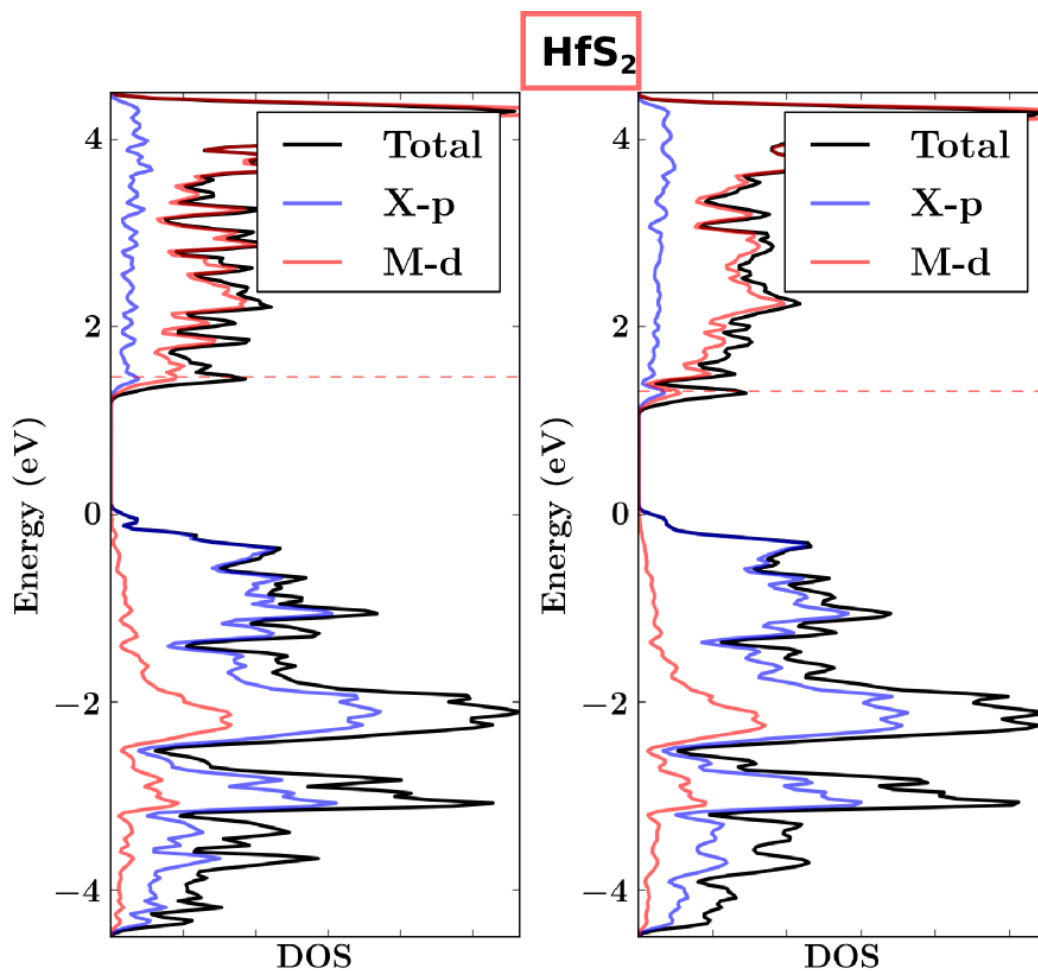


Figure S66: The left panel shows the DOS of the neutral  $\text{HfS}_2$  with sulfur vacancy and right panel corresponds to the same system when  $0.5 e^-$  is removed from the super cell. The nature of the DOS changes only slightly.

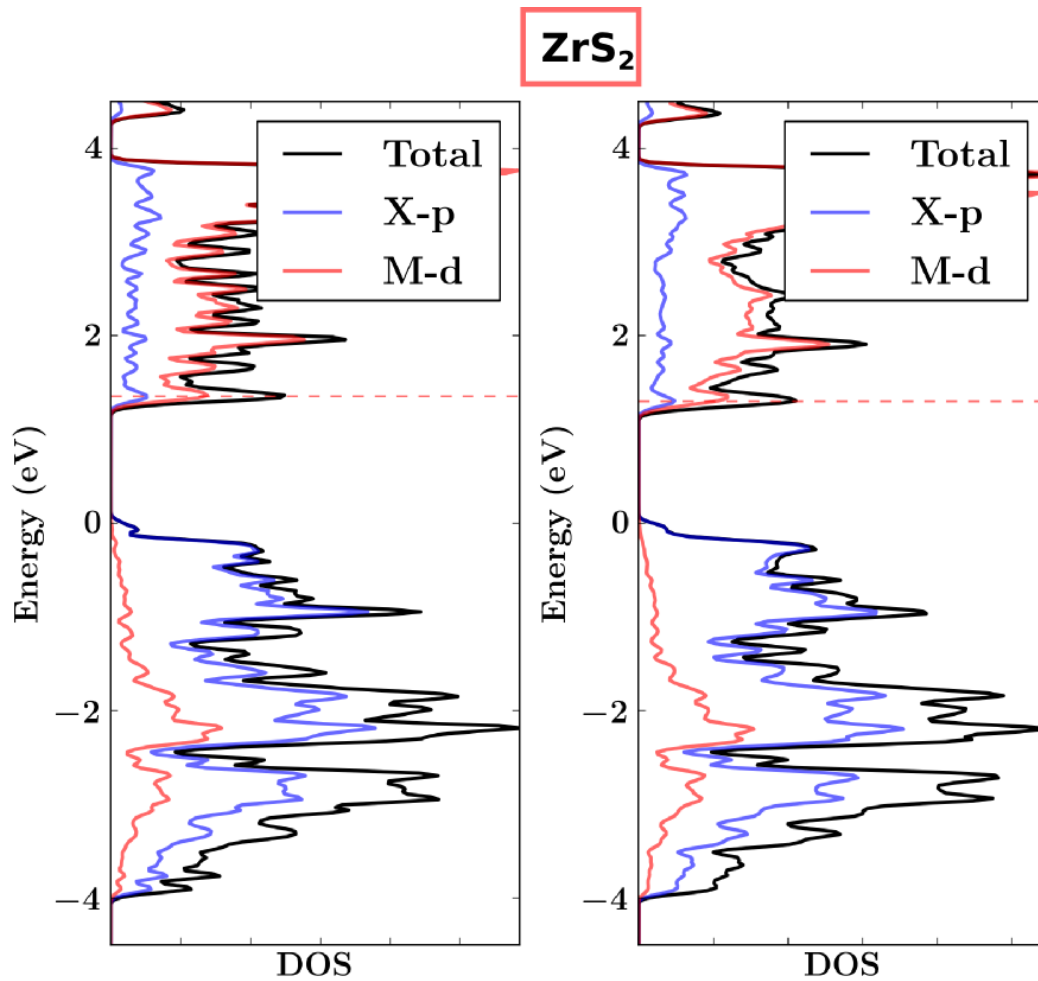


Figure S67: The left panel shows the DOS of the neutral ZrS<sub>2</sub> with sulfur vacancy and right panel corresponds to the same system when 0.5 e<sup>-</sup> is removed from the super cell. The nature of the DOS changes only slightly.

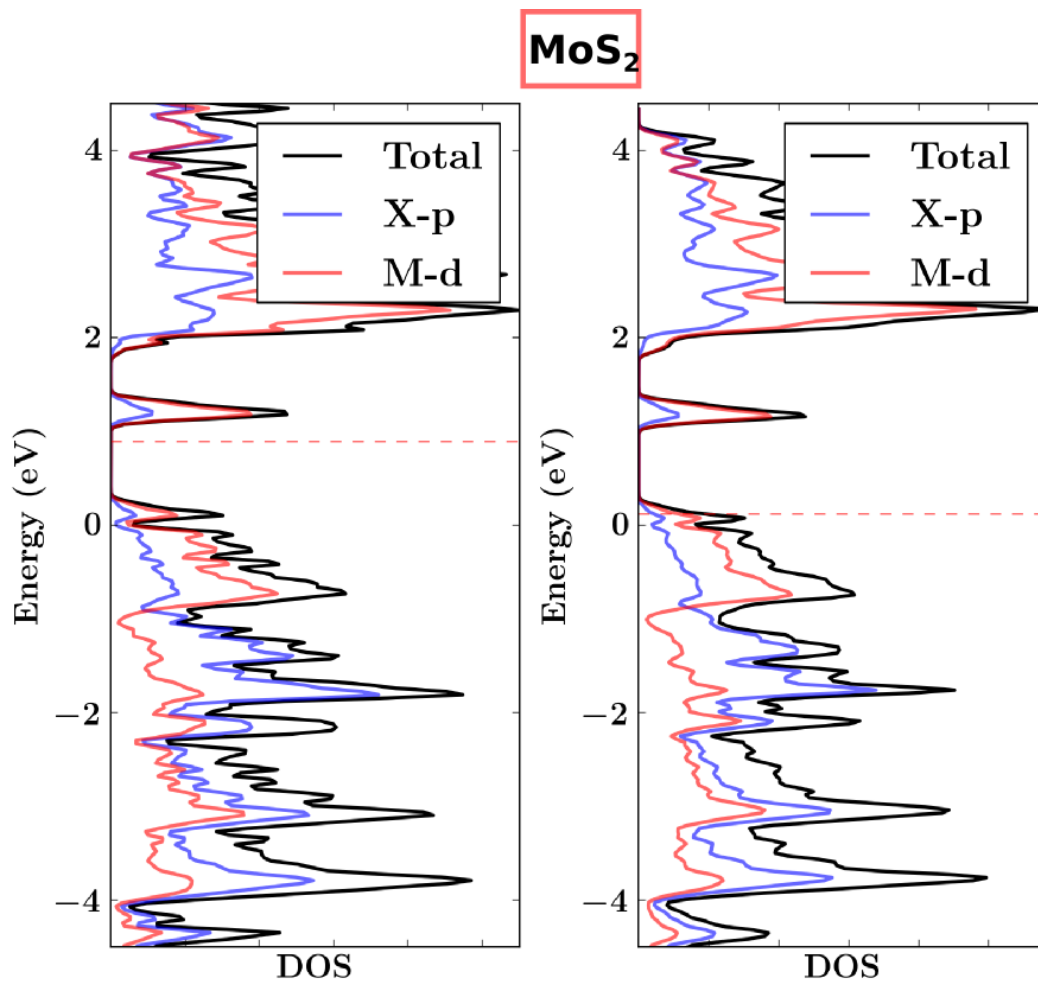


Figure S68: The left panel shows the DOS of the neutral MoS<sub>2</sub> with sulfur vacancy and right panel corresponds to the same system when 0.5 e<sup>-</sup> is removed from the super cell. The nature of the DOS changes only slightly.

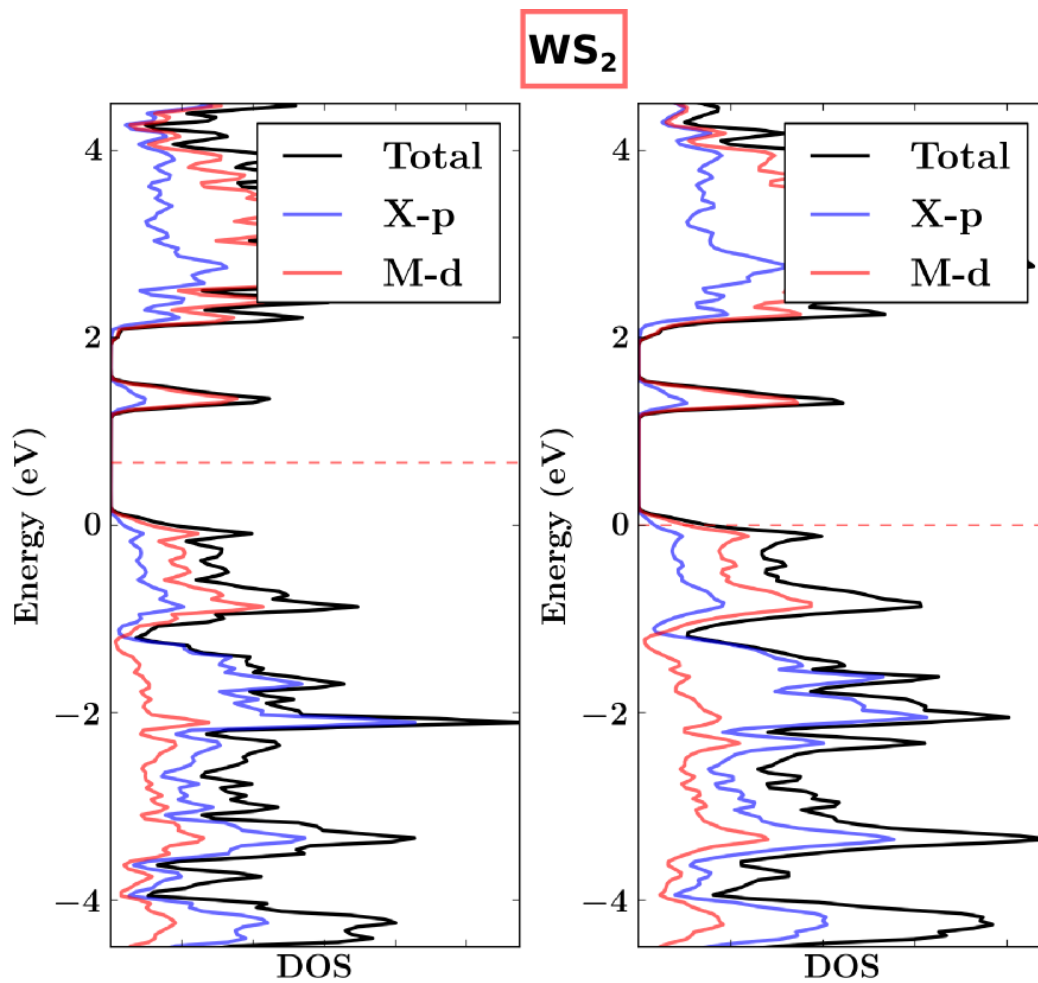


Figure S69: The left panel shows the DOS of the neutral WS<sub>2</sub> with sulfur vacancy and right panel corresponds to the same system when 0.5 e<sup>-</sup> is removed from the super cell. The nature of the DOS changes only slightly.

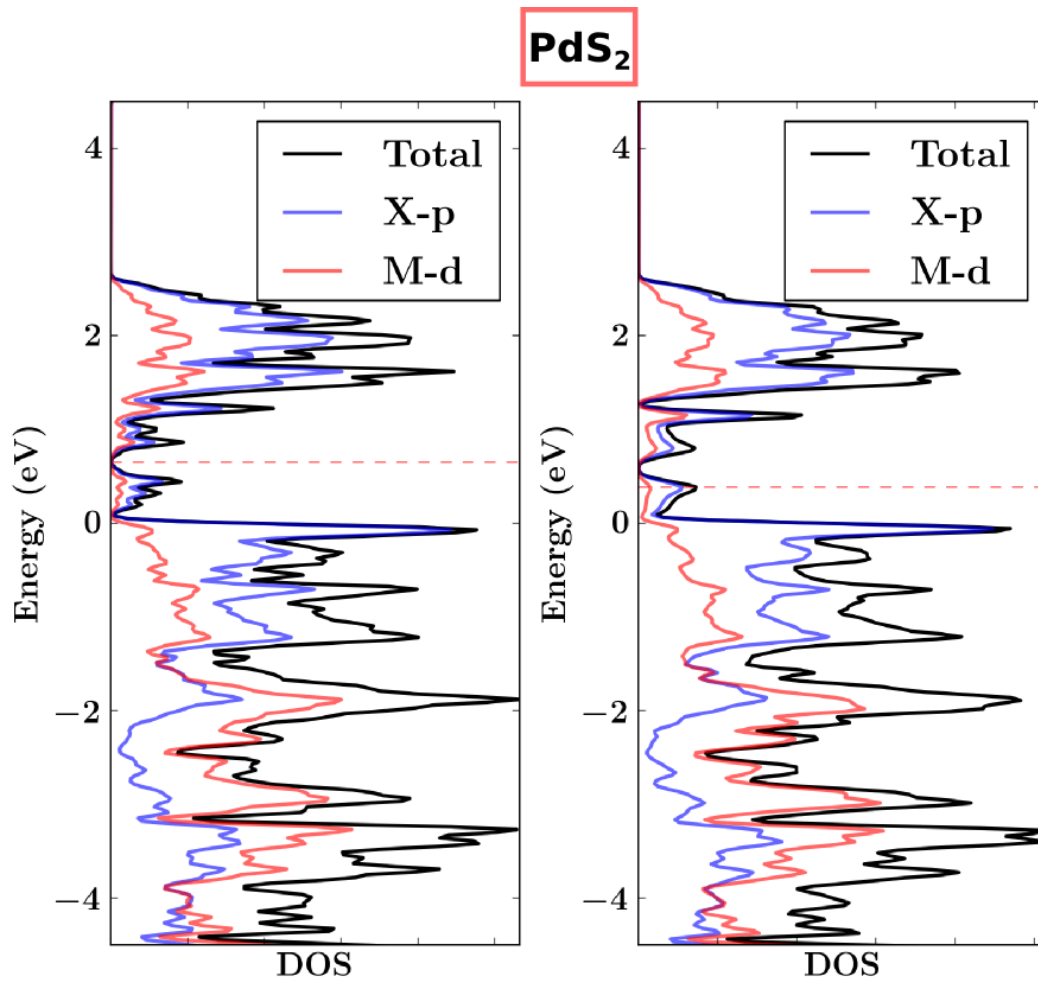


Figure S70: The left panel shows the DOS of the neutral PdS<sub>2</sub> with sulfur vacancy and right panel corresponds to the same system when 0.5 e<sup>-</sup> is removed from the super cell. The nature of the DOS changes only slightly.

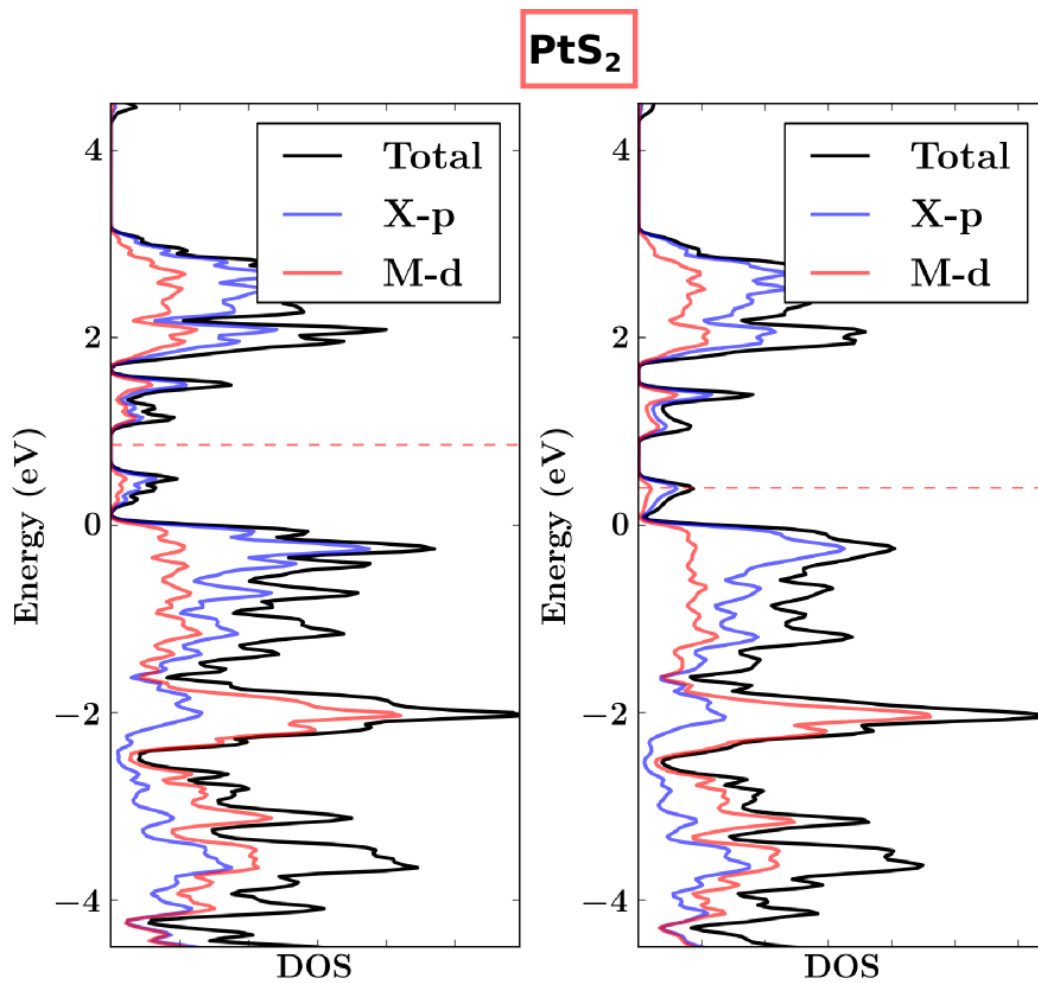


Figure S71: The left panel shows the DOS of the neutral PtS<sub>2</sub> with sulfur vacancy and right panel corresponds to the same system when 0.5 e<sup>-</sup> is removed from the super cell. The nature of the DOS changes only slightly.